Physica Scripta

ACCEPTED MANUSCRIPT

The response of a magnetic and dielectric cylinder subjected to an external magnetic and electric field of *any* form on the plane normal to the directional axis

To cite this article before publication: Petros Moraitis Moraitis *et al* 2025 *Phys. Scr.* in press https://doi.org/10.1088/1402-4896/adfd2c

The response of a magnetic and dielectric cylinder subjected to an external magnetic and electric field of *any* form on the plane normal to the directional axis

P. Moraitis, K. Tsakmakidis and D. Stamopoulos*
Department of Physics, School of Science, National and Kapodistrian University of Athens, Zografou Panepistimioupolis, 15784, Athens, Greece

*Author to whom correspondence should be addressed: e-mail: densta@phys.uoa.gr

Abstract
Here we report definite results on the mathematical metabolization of Maxwell's equations in one of the building units, most commonly met in practice. We investigate the static/quasi-static case of a linear, homogeneous and isotropic magnetic and dielectric cylinder of intrinsic susceptibility, χ^{int}, subjected to an *external* potential/field, $\mathcal{U}_{ext}/\mathcal{F}_{ext}$, of *any* form on the plane normal to the directional axis, produced by a primary source that resides at the outside space. Specifically, here we address analytically a magnetic and dielectric cylinder of seemingly infinite length along the z axis, subjected to an *external* potential/field, $\mathcal{U}_{ext}/\mathcal{F}_{ext}$, that does not vary along the z axis, as well. An expansion-based mathematical approach is employed, enabling direct access to universal expressions of the response of the magnetic and dielectric cylinder, i.e., the *internal* potential/field, $\mathcal{U}_{int}/\mathcal{F}_{int}$, produced by the secondary source of bound charges that is originally induced by the *external* potential/field, $\mathcal{U}_{ext}/\mathcal{F}_{ext}$. Accordingly, ready-to-use expressions of the *total* potential/field, $\mathcal{U}=\mathcal{U}_{ext}+\mathcal{U}_{int}/\mathcal{F}=\mathcal{F}_{ext}+\mathcal{F}_{int}$, and of the polarization, $\mathcal{P}$, of the magnetic and dielectric cylinder are directly obtained. These universal expressions are applicable to every distinct problem of different $\mathcal{U}_{ext}/\mathcal{F}_{ext}$, without the need to tackle it mathematically, every time, from the beginning. Interestingly, the depolarization factor, N, and extrinsic susceptibility, χ^{ext}, are degenerate, obtaining a constant value irrespectively of the mode of the *external* potential/field, $\mathcal{U}_{ext}/\mathcal{F}_{ext}$. These universal expressions between $\mathcal{U}_{int}$-$\mathcal{U}_{ext}$, $\mathcal{U}$-$\mathcal{U}_{ext}$, $\mathcal{F}_{int}$-$\mathcal{F}_{ext}$, $\mathcal{F}$-$\mathcal{F}_{int}$ and $\mathcal{P}$-$\mathcal{F}_{ext}$ provide effective means to understand, design and realize cylindrical building units with specific characteristics.

Keywords: dielectric cylinders; magnetic cylinders; electric polarization; magnetic polarization; dielectric wires; magnetic wires

I. Introduction

During the last decades spherical and cylindrical structures of dielectric and magnetic materials, either compact or hollow shells, are intensively studied theoretically since they are widely employed as building units in useful applications.

Regarding dielectric spherical and cylindrical structures, they are incorporated in applications that relate to scattering and shielding/cloaking [1-4], modeling and manipulation of colloidal particles and biological cells [5-10] etc. For instance, in [2] Loulas et al. studied the directional scattering by dielectric cylinders. By tailoring both the electric and magnetic polarizabilities of the cylinders and by using a sinusoidally decaying wave, the authors achieved significant backward scattering. In [4] Wu et al. investigated a dielectric cylinder covered by an invisibility cloak. The authors proved that the properties of the inner dielectric cylinder and of the outer

cloak should be matched appropriately to avoid the transmission of electric fields inside the dielectric cylinder. In [7] Zehe et al. studied aggregated human red blood cells in the form of rouleaux, thus approximated by dielectric cylinders. Specifically, they investigated the induced dipole moment of short cylinders which are free to move/rotate in a liquid conductive medium under the effect of an alternating external electric field. Interestingly, the authors considered the depolarization effect due to the secondary/bound electric charges that are induced at the rouleaux/dielectric cylinder. The polarization and the electro-rotation torque spectra of the rouleaux/dielectric cylinder were calculated in closed-form relations for the case of spatially-homogeneous, alternating external electric field. In [9] Ye et al. investigated the influence of an electric field transverse to a uniform, long and straight nerve axon stimulated by a time-varying, spatially-homogeneous magnetic field applied parallel to directional axis. To this effect, they employed an unmyelinated axon model and provided an analytic expression for the transmembrane potential, taking into account the characteristics of the externally applied magnetic field (e.g. magnitude, frequency etc) and the properties of the tissue (e.g. conductivity, susceptibility etc). In [10] Spreng et al. studied the electromagnetic Casimir interaction between two long dielectric cylinders placed inside a liquid ionic medium (i.e. salted water) to model processes observed in relevant biological systems, e.g. actin filaments and microtubules. The authors demonstrated that under specific biological conditions both entities form bundles through the involvement of relevant proteins, processes that can be reproduced on the basis of the Casimir interaction.

Referring to magnetic spherical and cylindrical structures, they are used in scattering and shielding/cloaking [11-14], environment [15,16], sorting/manipulation of biological cells [17-24], diagnosis and therapy in biomedicine [25-32] etc. For instance, in [12] Ma et al. studied an elliptic cylinder cloak realized by metamaterials of appropriate, position dependent, anisotropic electric and magnetic susceptibilities. The authors studied the efficiency of cloaking for different angles between the major axis of the elliptic cylinder and incident wave beam, evidencing that for the parallel/non-parallel case the cloaking effect is complete/incomplete. Evidently, when the major and minor axes of the elliptic cylinder are practically equal the authors obtained the results expected for the circular cylinder. In [21] the authors reviewed the synthesis and chemical, electrical, magnetic, and optical properties of high-aspect-ratio nanoparticles, i.e. rods, wires, and tubes of nano dimensions. These were exploited for the controlled engagement with cells and biomolecules in sensing, separation, and delivery applications. In [23] Cribb et al. investigated the magnetotransport behavior of spherical and cylindrical magnetic particles under controlled magnetophoretic conditions by using solutions of lambda-phage DNA as a host liquid medium. The obtained results are useful for therapeutic biomedical applications such as drug delivery and hyperthermia. In [24] Hultgren et al. reported on the experimental use of magnetic nanowires for cell separation purposes. Specifically, the authors employed NIH-3T3 mouse fibroblasts and Ni nanowires of 350 nm diameter and 35 μm length. The used cells had high affinity for binding to the hydrophilic layer of native oxide formed on the Ni nanowires. The authors demonstrated separation purity higher than 90% and yield of 49%. In [27] Zubarev et al. investigated hyperthermia theoretically, focusing on the production of heat by rod-like ferromagnetic nanoparticles hosted as a dilute suspension by a Maxwell viscoelastic liquid, when subjected to a linearly polarized ac magnetic field. The authors considered both mechanisms involved in the production of heat (i) the Brownian one, relating to the simultaneous rotation of each magnetic moment together with the host nanoparticle and (ii) the Néel one, referring to the rotation solely of each magnetic moment while the host nanoparticle preserves its original orientation. The

systematic study of all relevant parameters such as the shape and the magnetic susceptibility of the rod-like nanoparticles, together with the rheological properties of the liquid medium, enabled the authors to clarify the mechanisms that determine the efficacy of heat releasing. In [30] Wang et al. reported on the potential use of ferromagnetic hollow cylinders as contrast agents in magnetic resonance imaging. More specifically, micro/nano-scale hollow cylinders of iron oxide were fabricated due to their biocompatibility and tunability and proposed as potential contrast agents in magnetic resonance imaging. In [32] Hournkumnuard et al. focused on drug delivery by means of drug-carrying ferromagnetic nanoparticles that were captured by ferromagnetic microwires formerly implanted within blood vessels. To this effect an external spatially-homogeneous magnetic field was applied to magnetize the microwires and activate them as efficient magnetic traps for the retention of the drug-carrying magnetic nanoparticles. The authors evidenced that the retention effectiveness of the magnetic microwires was significantly improved when the spatially-homogeneous external magnetic field that was applied had strength on the order of 0.8 T.

Practically all the above works referred to the cases either of a spatially-homogeneous external electric/magnetic field or at high frequencies and were, mostly, computational. In the present work our motivation was to obtain analytical expressions for the more demanding general case where the external DC or low-frequency AC electric/magnetic field has *any* form, at least on the plane normal to the cylinder, while it preserves homogeneity only along the cylinder's axis. Except for its importance *per se*, such theoretical toolkit of analytical expressions will be useful for relevant applications.

Before proceeding with the analytical solution, we set the problem, we describe the overall employed approach and clarify the notation of the involved physical entities. Generally, in these cases, the dielectric and magnetic spheres and cylinders are exposed to an *external* potential, $\mathcal{U}_{ext}(\mathbf{r})$ (electric, $U_{ext}(\mathbf{r})$, and magnetic, $U_{m,ext}(\mathbf{r})$, respectively) that associates to the relevant *external* field, $\mathcal{F}_{ext}(\mathbf{r})$ (electric, $\mathbf{E}_{ext}(\mathbf{r})$, and magnetic, $\mathbf{H}_{ext}(\mathbf{r})$, respectively). It should be noted that $\mathcal{U}_{ext}(\mathbf{r})/\mathcal{F}_{ext}(\mathbf{r})$ are applied by the user and originate from a primary source (else, free source) that resides outside the spheres and cylinders. The response of the dielectric and magnetic spheres and cylinders is the *internal* potential, $\mathcal{U}_{int}(\mathbf{r})$ (electric, $U_{int}(\mathbf{r})$, and magnetic, $U_{m,int}(\mathbf{r})$, respectively) that relates to the relevant *internal* field, $\mathcal{F}_{int}(\mathbf{r})$ (electric, $\mathbf{E}_{int}(\mathbf{r})$, and magnetic, $\mathbf{H}_{int}(\mathbf{r})$, respectively). These *internal* entities originate from a secondary source (else, bound source) that resides at the spheres and cylinders [33-35]. The *total* potential, $\mathcal{U}(\mathbf{r})=\mathcal{U}_{ext}(\mathbf{r})+\mathcal{U}_{int}(\mathbf{r})$, and *total* field, $\mathcal{F}(\mathbf{r})=\mathcal{F}_{ext}(\mathbf{r})+\mathcal{F}_{int}(\mathbf{r})$, are obtained easily through the superposition principle [33-35]. It should be stressed that for any applied *external* potential/field, $\mathcal{U}_{ext}(\mathbf{r})/\mathcal{F}_{ext}(\mathbf{r})$, the physical entities of interest are the *internal* $\mathcal{U}_{int}(\mathbf{r})/\mathcal{F}_{int}(\mathbf{r})$ and *total* $\mathcal{U}(\mathbf{r})/\mathcal{F}(\mathbf{r})$ ones. These should be obtained throughout the whole space, i.e. both inside and outside the spheres and cylinders. The case of linear, homogeneous and isotropic dielectric and magnetic spheres was addressed mathematically in [36]. In that work [36] a series-based strategy was introduced that enabled us to obtain universal expressions for the *internal* $\mathcal{U}_{int}(\mathbf{r})/\mathcal{F}_{int}(\mathbf{r})$ and *total* $\mathcal{U}(\mathbf{r})/\mathcal{F}(\mathbf{r})$ potential/field and the polarization, $\mathcal{P}(\mathbf{r})$, of dielectric and magnetic spheres, literally, for *any* form of the *external* $\mathcal{U}_{ext}(\mathbf{r})/\mathcal{F}_{ext}(\mathbf{r})$, applied by the user.

Here, we focus on another standard case, that of the magnetic and dielectric cylinder (else, wire or filament), used in many applications as a building unit. Specifically, by using the Maxwells' equations we investigate a magnetic and dielectric cylinder coming from a linear, homogeneous and isotropic parent material of known *intrinsic* susceptibility, χ^{int} ($0 \leq \chi_e^{int}$ and $-1 \leq \chi_m^{int}$, respectively). The cylinder is of infinite length (else, its length, L, is orders of magnitude higher

than its diameter, $D = 2a$, see Figures 1(a)-1(b), 2 and 3, below) and is subjected to a DC *external* potential/field, $\mathcal{U}_{ext}(\mathbf{r})/\mathcal{F}_{ext}(\mathbf{r})$ (the results obtained here hold for the quasistatic case of an AC field of low-frequency, as well). As done in [36], here we aim to handle the most general case where the *external*, $\mathcal{U}_{ext}(\mathbf{r})/\mathcal{F}_{ext}(\mathbf{r})$, are of *any* form. However, in contrast to a sphere, the cylinder does not possess shape symmetry on both the azimuthal and polar angles. Thus, due to the luck of absolute shape symmetry here we study the case where the *external* potential/field, $\mathcal{U}_{ext}(\mathbf{r})/\mathcal{F}_{ext}(\mathbf{r})$, can have *any* form only on the plane normal to the directional axis of the cylinder (let us say z axis), while they preserve translational invariance along it. These are produced by a primary source (else, free source) that resides outside the cylinder and is handled by the user. Below, we find the *internal*, $\mathcal{U}_{int}(\mathbf{r})/\mathcal{F}_{int}(\mathbf{r})$, and *total*, $\mathcal{U}(\mathbf{r})/\mathcal{F}(\mathbf{r})$, entities, both inside and outside the magnetic and dielectric cylinder, together with its polarization, $\mathcal{P}(\mathbf{r})$ ($\mathbf{P}$ and $\mathbf{M}$, respectively). Our mathematical strategy metabolizes all lengthy calculations that are unavoidable by standard methods, enabling us to obtain universal and reliable expressions for all $\mathcal{U}_{int}(\mathbf{r})$, $\mathcal{F}_{int}(\mathbf{r})$, $\mathcal{U}(\mathbf{r})$, $\mathcal{F}(\mathbf{r})$ and $\mathcal{P}(\mathbf{r})$ that are applicable for *any* form of $\mathcal{U}_{ext}(\mathbf{r})/\mathcal{F}_{ext}(\mathbf{r})$, without the need to tackle each new problem from the beginning. This is fairly documented for a couple of representative cases met in the literature. Our universal expressions pave the way to understand and manipulate the response of magnetic and dielectric cylindrical units at will. This property can be useful in applications.

II. Materials and methods

Magnetite (Fe_3O_4) nano/micro-cylinders were synthesized by means of a hydrothermal route. Specifically, a stochiometric mixture of $FeSO_4 \cdot 7H_2O$ and $Na_2S_2O_3 \cdot 5H_2O$ is placed inside an autoclave preloaded with an aqueous solution of PEG of molecular weight 400 D (PEG/H_2O=1/9), then NaOH is added and the autoclave is exposed at a relatively low reaction temperature, T_{reac}=150 ^{0}C, for the desired duration, t_{reac}=24 h. All chemicals were purchased from Merck (Merck, Darmstadt, Germany) and were of purity above 99%.
Magnetization loops were obtained via a Superconducting Quantum Interference Device (SQUID) magnetometer, model MPMS 5.5T (Quantum Design, San Diego, CA, USA). Microscopy images were obtained via a Scanning Electron Microscope, model Quanta Inspect (FEI Technologies Inc, Hillsboro, OR, USA).

III. Magnetic cylinder -linear, homogeneous and isotropic- subjected to an external pseudopotential/field of *any* form

In this section we apply our approach in a detailed way for the case of a magnetic cylinder. The results for the dielectric cylinder are summarized in the next section. Both cases are investigated on the basis of the Maxwells' equations. The general case of a magnetic and dielectric cylinder is schematically presented in Figures 1(a)-1(b). Ideally, to claim independence from the position along the z axis, the cylinder should be infinite. In practice, the same claim is satisfied by a cylinder of finite length, L, and radius, a, under the condition, $L/a \gg 1$. In this case, the two edges of the cylinder should have negligible contribution in comparison to that of its extended, central part. The cylinder is subjected to an external potential/field, $\mathcal{U}_{ext}(\mathbf{r})/\mathcal{F}_{ext}(\mathbf{r})$, of *any* form, applied by the user through a primary source, i.e. free charge/current density, that is placed outside the cylinder (not shown in Figures 1(a)-1(b)).

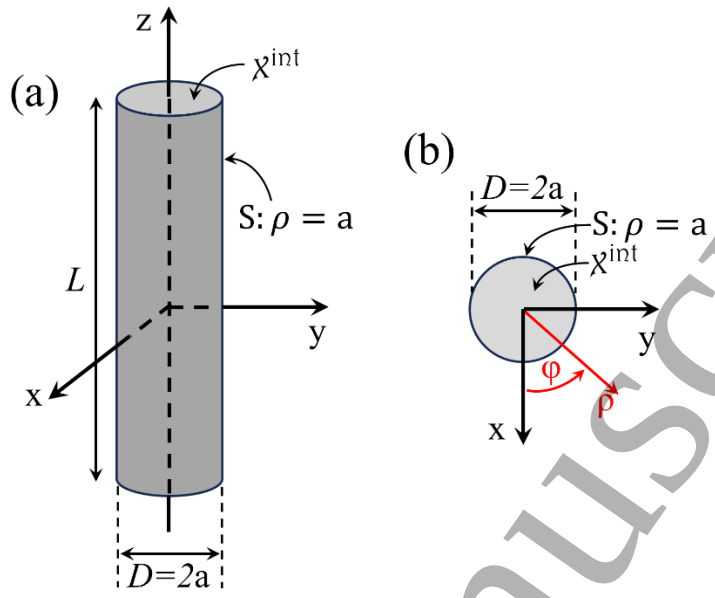

Figure 1. (a) Schematic presentation of a 3-dimensional cylinder of linear, homogeneous and isotropic parent material with intrinsic susceptibility, χ^{int}. The cylinder has length L and radius a (with $L/a \gg 1$) and is subjected to an external potential/field, $\mathcal{U}_{ext}(\mathbf{r})/\mathcal{F}_{ext}(\mathbf{r})$. The potential/field can have *any* form of inhomogeneity on the normal x-y plane, however, is homogeneous along the directional axis (cylinder's axis, z). (b) Schematic presentation of the cylinder on the x-y plane. Due to the independence of both the cylinder's properties and of the external potential/field, $\mathcal{U}_{ext}(\mathbf{r})/\mathcal{F}_{ext}(\mathbf{r})$, from the position along the z axis, the original 3-dimensional problem is actually 2-dimensional.

Here we investigate the case where the primary source is homogenous along the z axis, so that the produced external potential/field, $\mathcal{U}_{ext}(\mathbf{r})/\mathcal{F}_{ext}(\mathbf{r})$, are independent of z, as well. In addition, the cylinder is compact, has radius a, and consists of linear, homogeneous and isotropic material of intrinsic susceptibility, χ^{int} (i.e., $0 \leq \chi_e^{int}$ for a dielectric material and $-1 \leq \chi_m^{int}$ for a magnetic material). The external $\mathcal{U}_{ext}(\mathbf{r})/\mathcal{F}_{ext}(\mathbf{r})$ induce secondary sources, i.e. bound charge and pseudocharge densities, that reside at the cylinder. In the general case, the induced bound pseudocharges and charges are both volume ($\rho_{m,b}(\mathbf{r}) = -\nabla \cdot \mathbf{M}(\mathbf{r})$ and $\rho_b(\mathbf{r}) = -\nabla \cdot \mathbf{P}(\mathbf{r})$) and surface ($\sigma_{m,b}(\mathbf{r}) = (\mathbf{M}(\mathbf{r}) \cdot \hat{\mathbf{n}})|_{S:\rho=a}$ and $\sigma_b(\mathbf{r})|_{\rho=a} = (\mathbf{P}(\mathbf{r}) \cdot \hat{\mathbf{n}})|_{S:\rho=a}$) ones, due to the, possibly, volume-nonhomogeneous and, surely, surface-discontinuous behavior of the polarization, $\mathcal{P}(\mathbf{r})$ ($\mathbf{M}$ and $\mathbf{P}$, respectively) [33-35]. Here, $\rho_{m,b}(\mathbf{r}) = \rho_b(\mathbf{r}) = 0$ due to the homogeneous nature of the cylinder. Thus, in our case the only secondary source is the $\sigma_{m,b}(\mathbf{r})$ and $\sigma_b(\mathbf{r})$, induced at the surface of the cylinder, S: ρ = a. Accordingly, depending on the magnetic and dielectric case, $\sigma_{m,b}(\mathbf{r})$ and $\sigma_b(\mathbf{r})$, will produce the internal potential/field, $\mathcal{U}_{int}(\mathbf{r})/\mathcal{F}_{int}(\mathbf{r})$, as a response of the cylinder to the external potential/field, $\mathcal{U}_{ext}(\mathbf{r})/\mathcal{F}_{ext}(\mathbf{r})$. Taking into account the above information, in our case the 3-dimensional problem, Figure 1(a), obtains a 2-dimensional character, Figure 1(b), while the internal $\mathcal{U}_{int}(\mathbf{r})/\mathcal{F}_{int}(\mathbf{r})$ depend only on the polar coordinates, so that they become $\mathcal{U}_{int}(\rho,\varphi)/\mathcal{F}_{int}(\rho,\varphi)$.

The conditions discussed above are realistic and can be met in a plethora of applications. For instance, in Figure 2 we show results for the magnetic case. Specifically, we show a

magnetization loop, $m(H_{ext})$, and a representative scanning electron microscopy image for a sample of magnetite (Fe_3O_4) in the form of nano/micro-cylinders.

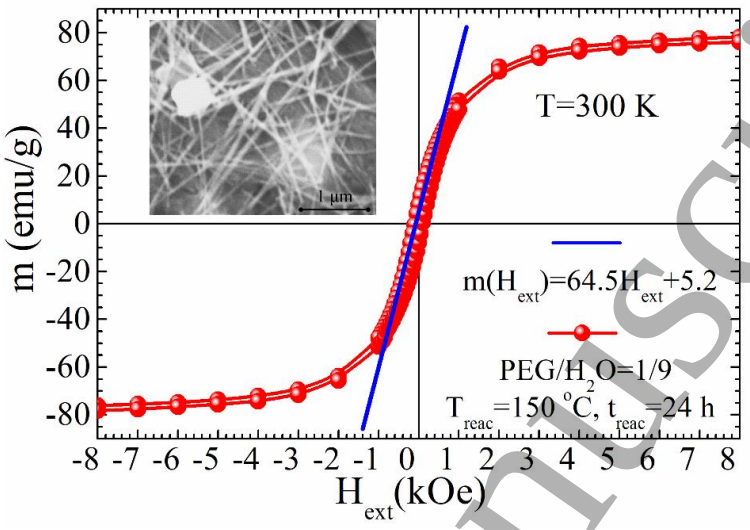

Figure 2. Isothermal SQUID DC magnetization loop as function of external magnetic field, H_{ext}, obtained at room temperature, T=300 K, for a sample of magnetite (Fe_3O_4) nano/micro-cylinders. The magnetization data obtained at low values of H_{ext} (i.e., within $-0.6\ \text{kOe} \leq H_{ext} \leq 0.6\ \text{kOe}$) can be reproduced by a linear fit shown by the blue, thick, straight line. The inset shows a representative SEM image of the magnetite nano/micro-cylinders.

The results of Figure 2 document two important things. First, the magnetization data obtained at low values of H_{ext} (i.e., within $-0.6\ \text{kOe} \leq H_{ext} \leq 0.6\ \text{kOe}$) can be reproduced quite effectively by a linear fit. This is shown by the blue, thick, straight line, $m(H_{ext}) = 64.5H_{ext} + 5.2$ ([m]=emu/g, while [H_{ext}]=kOe). Thus, the magnetite nano/micro-cylinders exhibit an almost linear constitutive relation, $m(H_{ext})$, at least in the regime prior to saturation. Second, from the SEM image of the inset we infer that the typical values of the length, L, and radius, a, of the magnetite nano/micro-cylinders range within $1\ \mu\text{m} \leq L \leq 30\ \mu\text{m}$ and $20\ \text{nm} \leq 2a \leq 200\ \text{nm}$. Thus, in these samples the condition $L/a \gg 1$ is satisfied. By taking into account both the magnetic behavior and the microstructure, these magnetite nano/micro-cylinders is a nice model system for the magnetic case.

Another model system that fits the subject of the present work comes from the field of superconductivity, since in the Meissner state, i.e., below the lower critical field, H_{c1}, the superconductors behave diamagnetically in an absolutely linear way on the external applied field, H_{ext}. For energy applications and for the production of high magnetic fields, composite wires that consist of both superconductors and normal metals are of particular interest. Figure 3 shows data for the case of Nb nano/micro-cylinders (else, nano/micro-wires and nano/micro-filaments) employed in the realization of composite Cu-Nb wires [37,38]. The SEM image of the inset shows the Cu-free, bare Nb nano/micro-cylinders when the Cu matrix has been removed through exposition to nitric acid for a few minutes [37]. The magnetization loops of the main panel were obtained for a Cu-15%Nb wire at $T = 4.5\ \text{K} < T_C$ and show comparatively the behavior of the original Cu-15%Nb wire and of the bare Nb nano/micro-cylinders after dissolution of the Cu matrix. We see that the bare Nb nano/micro-cylinders behave linearly on the external magnetic field, H_{ext} (in the original Cu-15%Nb wire, the presence of the Cu matrix

adds an extra magnetization peak observed at H^*, due to the proximity effect [38]). Accordingly, the magnetization of the bare Nb nano/micro-cylinders for $H_{ext} \leq H_{c1}$ (i.e., within $0 \leq H_{ext} \leq 1.1$ kOe) is nicely described by a linear fit as shown by the blue, thick, straight line, $m_{nor}(H_{ext}) = -0.83 \times 10^{-3} H_{ext} - 0.45 \times 10^{-3}$ (m_{nor} is dimensionless, while $[H_{ext}]$=kOe). Thus, the bare Nb nano/micro-cylinders for $H_{ext} \leq H_{c1}$ exhibit a linear constitutive relation, $m(H_{ext})$. Also, these bare Nb nano/micro-cylinders have ideal size characteristics since their length, L, exceeds by many orders of magnitude their radius, a, so that the condition $L/a \gg 1$ is surely satisfied.

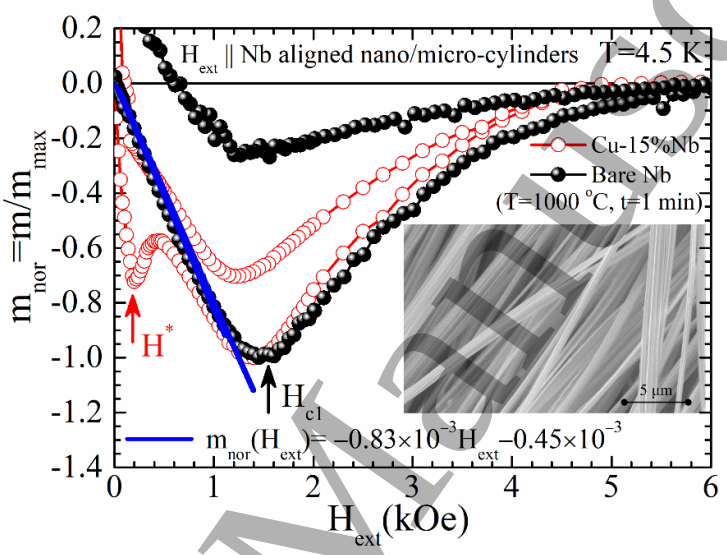

Figure 3. Isothermal SQUID DC magnetization loops as function of external magnetic field, H_{ext}, obtained at temperature $T = 4.5$ K $< T_C$ for a Cu-15%Nb wire (red open circles) and for the Cu-free, bare Nb nano/micro-cylinders (black spheres) after dissolution of the Cu matrix by means of nitric acid. The magnetization data obtained for the bare Nb nano/micro-cylinders at $H_{ext} \leq H_{c1}$ (i.e., within $0 \leq H_{ext} \leq 1.1$ kOe) are reproduced by a linear fit shown by the blue, thick, straight line. The inset shows a representative SEM image of the bare Nb nano/micro-cylinders. Both SQUID and SEM data are reproduced from [37,38].

Returning to the mathematical part, in the rest of this section we apply our method, with all necessary details, on the magnetic cylinder. The results for the dielectric cylinder are summarized, in brief, in the next section. Before proceeding, we have to note an important issue that relate in all these cases, that of the depolarization process. The limited size of all realistic specimens, inevitably results in a discontinuity in the polarization, $\mathcal{P}(\mathbf{r})$, at their surface. Thus, electric and magnetic poles, i.e., bound charges and pseudocharges, always appear at the surface. These secondary sources produce an internal potential/field, $\mathcal{U}_{int}(\mathbf{r})/\mathcal{F}_{int}(\mathbf{r})$ (else, depolarization field) that acts against the external ones, $\mathcal{U}_{ext}(\mathbf{r})/\mathcal{F}_{ext}(\mathbf{r})$, tending to depolarize the specimen. The internal entities, $\mathcal{U}_{int}(\mathbf{r})/\mathcal{F}_{int}(\mathbf{r})$, relate to the external ones, $\mathcal{U}_{ext}(\mathbf{r})/\mathcal{F}_{ext}(\mathbf{r})$, through the so-called extrinsic susceptibility, χ^{ext}, and depolarization factor, N [39-42]. Finding closed-form expressions for these entities, whenever possible, is of paramount importance for applications (see below).

For the magnetic cylinder discussed in this section, the total pseudopotential/field, $U_m(\mathbf{r})/\mathbf{H}(\mathbf{r})$, are given by the following relations [33-35]

$$\mathrm{U_m}(\mathbf{r}) = \mathrm{U_{m,ext}}(\mathbf{r}) + \mathrm{U_{m,int}}(\mathbf{r}) \tag{1}$$

and

$$\mathbf{H}(\mathbf{r}) = \mathbf{H}_{\mathrm{ext}}(\mathbf{r}) + \mathbf{H}_{\mathrm{int}}(\mathbf{r}) \tag{2}$$

We note that here we investigate the most general case where the external $\mathrm{U_{m,ext}}(\mathbf{r})/\mathbf{H}_{\mathrm{ext}}(\mathbf{r})$ can be of *any* form on the plane normal to z axis, however, being homogeneous along it. Under these circumstances, by solving the Laplace equation and using the separation of variables technique [33-35], $\mathrm{U_{m,ext}}(\mathbf{r}) = \mathrm{U_{m,ext}}(\rho)\mathrm{U_{m,ext}}(\varphi)$, we get

$$\frac{\rho}{\mathrm{U_{m,ext}}(\rho)}\frac{\mathrm{d}}{\mathrm{d}\rho}\left(\rho\frac{\mathrm{dU_{m,ext}}(\rho)}{\mathrm{d}\rho}\right) + \frac{1}{\mathrm{U_{m,ext}}(\varphi)}\frac{\mathrm{d^2U_{m,ext}}(\varphi)}{\mathrm{d}\varphi^2} = 0 \tag{3}$$

The differential equation with respect to, φ, is equal to, $-\mathrm{n}^2 < 0$, where, $\mathrm{n} \in \mathrm{R}$, since its solution must be periodic (our problem is defined in the entire range, $0 \le \varphi \le 2\pi$), while the differential equation with respect to, ρ, is equal to, $+\mathrm{n}^2 > 0$, as relation (3) dictates. This means that for the, angular component, $\mathrm{U_{m,ext}}(\varphi)$, we get [33-35]

$$\mathrm{U_{m,ext}}(\varphi) = \begin{cases} \mathrm{A_{0,m}} + \mathrm{B_{0,m}}\varphi, & \mathrm{n} = 0 \\ \mathrm{A_{n,m}}\cos(\mathrm{n}\varphi) + \mathrm{B_{n,m}}\sin(\mathrm{n}\varphi), & \mathrm{n} \neq 0 \end{cases} \tag{4}$$

Using the boundary condition, $\mathrm{U_{m,ext}}(\varphi) = \mathrm{U_{m,ext}}(\varphi + 2\pi)$, we get that, $\mathrm{B_{0,m}} = 0$, from, $\mathrm{n} = 0$ and $\mathrm{n} \in \mathrm{Z}$, from, $\mathrm{n} \neq 0$, thus relation (4) becomes

$$\mathrm{U_{m,n,ext}}(\varphi) = \mathrm{A_{n,m}}\cos(\mathrm{n}\varphi) + \mathrm{B_{n,m}}\sin(\mathrm{n}\varphi), \quad \mathrm{n} \in \mathrm{Z} \tag{5}$$

Similarly, the radial component, $\mathrm{U_{m,ext}}(\rho)$, becomes [33-35]

$$\mathrm{U_{m,n,ext}}(\rho) = \begin{cases} \mathrm{C_{0,m}} + \mathrm{D_{0,m}}\ln\rho, & \mathrm{n} = 0 \\ \mathrm{C_{n,m}}\rho^{\mathrm{n}} + \mathrm{D_{n,m}}\rho^{-\mathrm{n}}, & \mathrm{n} \in \mathrm{Z} - \{0\} \end{cases} \tag{6}$$

Here we recall that the primary source that produces the external pseudopotential/field, $\mathrm{U_{m,ext}}(\mathbf{r})/\mathbf{H}_{\mathrm{ext}}(\mathbf{r})$, is placed outside the magnetic cylinder. Accordingly, using the condition that, $\mathrm{U_{m,ext}}(\rho)$, must be finite at, $\rho = 0$, we get that, $\mathrm{D_{0,m}} = 0$, from, $\mathrm{n} = 0$ and $\mathrm{D_{n,m}} = 0$, from, $\mathrm{n} \in \mathrm{Z} - \{0\}$, thus, relation (6) becomes

$$\mathrm{U_{m,n,ext}}(\rho) = \mathrm{C_{n,m}}\rho^{\mathrm{n}}, \qquad \mathrm{n} = 1,2,3,\ldots,\infty \tag{7}$$

By combining relations (5) and (7) we get that the general solution of, $\mathrm{U_{m,ext}}(\mathbf{r})$, is given by

$$\mathrm{U_{m,ext}}(\mathbf{r}) = \sum_{\mathrm{n}=0}^{\infty}\mathrm{U_{m,n,ext}}(\mathbf{r}) = \mathrm{A_{0,m}} + \sum_{\mathrm{n}=1}^{\infty}\rho^{\mathrm{n}}\left(\mathrm{A_{n,m}}\cos(\mathrm{n}\varphi) + \mathrm{B_{n,m}}\sin(\mathrm{n}\varphi)\right) \tag{8}$$

where we renamed the coefficients, $A_{n,m}C_{n,m} \to A_{n,m}$ and $B_{n,m}C_{n,m} \to B_{n,m}$, for every, n. The general term of the expansion is defined as

$$U_{m,n,ext}(\mathbf{r}) = \rho^n\left(A_{n,m}\cos(n\varphi) + B_{n,m}\sin(n\varphi)\right) \tag{9}$$

Similarly, $\mathbf{H}_{ext}(\mathbf{r})$, due to the constitutive relation $\mathbf{H}_{ext}(\mathbf{r}) = -\boldsymbol{\nabla}U_{m,ext}(\mathbf{r})$, should follow the respective expansion

$$\mathbf{H}_{ext}(\mathbf{r}) = \sum_{n=1}^{\infty}\mathbf{H}_{n,ext}(\mathbf{r}) = -\sum_{n=1}^{\infty}\boldsymbol{\nabla}\left(\rho^n\left(A_{n,m}\cos(n\varphi) + B_{n,m}\sin(n\varphi)\right)\right) \tag{10}$$

Note that in the above relation we have rejected the term, $n = 0$, since it obviously equals zero. The general term of the expansion is defined as

$$\mathbf{H}_{n,ext}(\mathbf{r}) = -\boldsymbol{\nabla}\left(\rho^n\left(A_{n,m}\cos(n\varphi) + B_{n,m}\sin(n\varphi)\right)\right) \tag{11}$$

It should be noted that the above expressions of the external $U_{m,ext}(\mathbf{r})/\mathbf{H}_{ext}(\mathbf{r})$ hold for both the inside and outside space of the cylinder, $\mathbf{H}_{ext}(\mathbf{r}) = \mathbf{H}_{ext}^{in}(\mathbf{r}) = \mathbf{H}_{ext}^{out}(\mathbf{r})$. In these expressions, the coefficients, $A_{n,m}$ and $B_{n,m}$, are given by

$$A_{0,m} = \frac{1}{2\pi}\int_0^{2\pi}U_{m,ext}(\mathbf{r})d\varphi \tag{12}$$

$$A_{n,m} = \frac{1}{\pi\rho^n}\int_0^{2\pi}U_{m,ext}(\mathbf{r})\cos(m\varphi)\,d\varphi \tag{13}$$

$$B_{n,m} = \frac{1}{\pi\rho^n}\int_0^{2\pi}U_{m,ext}(\mathbf{r})\sin(m\varphi)\,d\varphi \tag{14}$$

Notice that in the above coefficients the first subscript, n, refers to the order of the mode/term, while the second subscript, m, denotes the magnetic case studied here. The mode/term $n = 0$ is not considered below since it refers to a constant pseudopotential/zero field. The expansion coefficients, $A_{n,m}$ and $B_{n,m}$, seem to be functions of the radial coordinate, ρ. However, recalling that $U_{m,ext}(\mathbf{r})$ obeys the separation of variables, $U_{m,ext}(\mathbf{r}) \sim U_{m,ext}(\rho)U_{m,ext}(\varphi)$, we easily see that the radial component, $U_{m,ext}(\rho)$, can be brought out of the integral. Accordingly, the term $1/\rho^n$ is ultimately cancelled so that the expansion coefficients, $A_{n,m}$ and $B_{n,m}$, become constants.

Once we have defined the form of the external entities, $U_{m,ext}(\mathbf{r})/\mathbf{H}_{ext}(\mathbf{r})$, we may focus on the internal ones, $U_{m,int}(\mathbf{r})/\mathbf{H}_{int}(\mathbf{r})$, which are produced by the secondary source of surface bound pseudocharge, $\sigma_{m,b}(\mathbf{r}) = (\mathbf{M}(\mathbf{r})\cdot\hat{\mathbf{n}})|_{S:\rho=a}$, due to the respective discontinuity of the magnetization, $\mathbf{M}(\mathbf{r}) = \chi_m^{int}\mathbf{H}(\mathbf{r})$ (in our case $\boldsymbol{\nabla}\cdot\mathbf{M}(\mathbf{r}) = 0$ so that volume bound pseudocharges

do not exist). Under these conditions, the internal scalar potential, $U_{m,int}(\mathbf{r})$, is obtained from $\sigma_{m,b}(\mathbf{r})$ through the generalized law of Coulomb [33-35], which due to the cylindrical character of the problem becomes [43]

$$U_{m,int}(\mathbf{r}) = -\frac{a}{2\pi}\int_0^{2\pi} \sigma_{m,b}(\mathbf{r}')\ln|\boldsymbol{\rho} - a\hat{\boldsymbol{\rho}}'|\,d\varphi' = -\frac{a}{2\pi}\int_0^{2\pi} (\mathbf{M}(\mathbf{r}')\cdot\hat{\boldsymbol{\eta}}')\ln|\boldsymbol{\rho} - a\hat{\boldsymbol{\rho}}'|\,d\varphi' \quad (15)$$

Notice that in the specific 2-dimensional case studied here, the pseudocharge density is actually linear, $\lambda_{m,b}(a,\varphi')$, since it resides along the periphery of the slice of the cylinder, $\rho' = a$, as shown in Figure 1(b). However, since in the general case any pseudocharge density should depend on $\mathbf{r}' = (\rho',\varphi')$, we will keep using the more general symbol $\sigma_{m,b}(\mathbf{r}')$. The above integral can be modified based on the multipole expansion on the basis of $\cos(n\varphi)$ and $\sin(n\varphi)$. Since we are interested in finding the total magnetic field everywhere in space, we should employ the proper expansion of $\ln|\boldsymbol{\rho} - \boldsymbol{\rho}'|$ in each one of the two cases of interest, that is for the inside space ($\rho < \rho'$) and outside space ($\rho' < \rho$). For the general case, these expansions are given by [44]

$$\ln|\boldsymbol{\rho} - \boldsymbol{\rho}'| = \ln\rho' - \sum_{n=1}^{\infty}\frac{1}{n}\left(\frac{\rho}{\rho'}\right)^n \cos[n(\varphi - \varphi')]\,, \quad \rho < \rho' \quad (16)$$

and

$$\ln|\boldsymbol{\rho} - \boldsymbol{\rho}'| = \ln\rho - \sum_{n=1}^{\infty}\frac{1}{n}\left(\frac{\rho'}{\rho}\right)^n \cos[n(\varphi - \varphi')]\,, \quad \rho' < \rho \quad (17)$$

where ρ and ρ' run over the volume of observation and sources, respectively. In our case, the sources refer to the secondary/bound charge, $\sigma_{m,b}(\mathbf{r}')$, that resides at $\rho' = a$. Combining relations (16) and (17) with relation (15), and using the facts that the coordinates of the secondary/bound source are, $\mathbf{r}' = (\rho',\varphi') = (a,\varphi')$ and that the normal vector to the surface of the cylinder is, $\hat{\boldsymbol{\eta}}' = \hat{\boldsymbol{\rho}}'$, we get for the internal scalar pseudopotential

$$U^{in}_{m,int}(\mathbf{r}) = -\frac{a\ln a}{2\pi}\int_0^{2\pi}\mathbf{M}(a,\varphi')\cdot\hat{\boldsymbol{\rho}}'d\varphi' + \frac{a}{2\pi}\sum_{n=1}^{\infty}\frac{1}{n}\left(\frac{\rho}{a}\right)^n\int_0^{2\pi}\mathbf{M}(a,\varphi')\cdot\hat{\boldsymbol{\rho}}'\cos[n(\varphi-\varphi')]\,d\varphi' \quad (18)$$

at the inside space of the cylinder, $\rho < a$ and

$$U^{out}_{m,int}(\mathbf{r}) = -\frac{a\ln\rho}{2\pi}\int_0^{2\pi}\mathbf{M}(a,\varphi')\cdot\hat{\boldsymbol{\rho}}'d\varphi' + \frac{a}{2\pi}\sum_{n=1}^{\infty}\frac{1}{n}\left(\frac{a}{\rho}\right)^n\int_0^{2\pi}\mathbf{M}(a,\varphi')\cdot\hat{\boldsymbol{\rho}}'\cos[n(\varphi-\varphi')]\,d\varphi' \quad (19)$$

at the outside space of the cylinder, $\rho > a$. For convenience, we define the integrals of relations (18) and (19) through the following relation

$$I_n^{in}(\varphi) = I_n^{out}(\varphi) = I_n(\varphi) = \int_0^{2\pi} \mathbf{M}(a,\varphi') \cdot \hat{\boldsymbol{\rho}}' \cos[n(\varphi - \varphi')]\, d\varphi' \tag{20}$$

Accordingly, the above relations (18) and (19) become

$$U_{m,int}^{in}(\mathbf{r}) = -\frac{a \ln a}{2\pi} I_0 + \frac{a}{2\pi} \sum_{n=1}^{\infty} \frac{1}{n} \left(\frac{\rho}{a}\right)^n I_n(\varphi) \tag{21}$$

and

$$U_{m,int}^{out}(\mathbf{r}) = -\frac{a \ln \rho}{2\pi} I_0 + \frac{a}{2\pi} \sum_{n=1}^{\infty} \frac{1}{n} \left(\frac{a}{\rho}\right)^n I_n(\varphi) \tag{22}$$

Realizing that the term I_0 is constant, the internal component of the magnetic field gets the form

$$\mathbf{H}_{int}^{in}(\mathbf{r}) = -\frac{a}{2\pi} \sum_{n=1}^{\infty} \frac{1}{n a^n} \nabla\left(\rho^n I_n(\varphi)\right) \tag{23}$$

for the inside space of the cylinder, $\rho < a$, and

$$\mathbf{H}_{int}^{out}(\mathbf{r}) = \frac{a I_0}{2\pi} \nabla(\ln \rho) - \frac{a}{2\pi} \sum_{n=1}^{\infty} \frac{a^n}{n} \nabla\left(\rho^{-n} I_n(\varphi)\right) \tag{24}$$

for the outside space of the cylinder, $\rho > a$.

Up to now we have found expansion-based expressions of the external and internal pseudopotential and field, throughout the whole space. However, we still need the expressions of the integrals, $I_n(\varphi)$, which are the same for the inside and outside space of the cylinder, as relation (20) evidences. Accordingly, we have to calculate the secondary source of bound pseudocharges, $\sigma_{m,b}(a,\varphi') = \mathbf{M}(a,\varphi') \cdot \hat{\boldsymbol{\rho}}'$. To this end, we argue that due to the linear character of the magnetic cylinder, at the inside space the total field is given by the relation

$$\mathbf{H}^{in}(\mathbf{r}) = \sum_{n=0}^{\infty} \mathbf{H}_n^{in}(\mathbf{r}) = \sum_{n=0}^{\infty} C_{n,m} \mathbf{H}_{n,ext}^{in}(\mathbf{r}) \tag{25}$$

where $C_{n,m}$ are the expansion coefficients, to be determined (notice that the first subscript, n, refers to the order of the mode/term, while the second subscript, m, denotes the magnetic case). With the help of relation (25) and considering that, $\mathbf{M}(\mathbf{r}) = \chi_m^{int} \mathbf{H}^{in}(\mathbf{r})$, we calculate

$$\sigma_{m,b}(a,\varphi') = \mathbf{M}(a,\varphi') \cdot \hat{\boldsymbol{\rho}}' = \chi_m^{int} \sum_{n'=0}^{\infty} C_{n',m} \mathbf{H}_{n',ext}^{in}(a,\varphi') \cdot \hat{\boldsymbol{\rho}}' \tag{26}$$

Substituting relation (10) into (26) we get

$$\sigma_{m,b}(a,\varphi') = -\chi_m^{int}\sum_{n'=0}^{\infty} C_{n',m}\left(\boldsymbol{\nabla}\left(\rho'^{n'}\left(A_{n',m}\cos(n'\varphi') + B_{n',m}\sin(n'\varphi')\right)\right)\cdot\hat{\boldsymbol{\rho}}'\right)|_{\rho'=a} \quad (27)$$

else

$$\sigma_{m,b}(a,\varphi') = -\chi_m^{int}\sum_{n'=0}^{\infty} C_{n',m}n'a^{n'-1}\left(A_{n',m}\cos(n'\varphi') + B_{n',m}\sin(n'\varphi')\right) \quad (28)$$

Now we substitute this result into relation (20) and we use the fact that, $\cos[n(\varphi-\varphi')] = \cos(n\varphi)\cos(n\varphi') + \sin(n\varphi)\sin(n\varphi')$. After performing the trigonometric integrals we get

$$I_n(\varphi) = -\chi_m^{int}\sum_{n'=0}^{\infty} C_{n',m}n'a^{n'-1}\pi\delta_{nn'}\left(A_{n',m}\cos(n\varphi) + B_{n',m}\sin(n\varphi)\right) \quad (29)$$

else

$$I_n(\varphi) = -\pi\chi_m^{int}C_{n,m}\,na^{n-1}\left(A_{n,m}\cos(n\varphi) + B_{n,m}\sin(n\varphi)\right) \quad (30)$$

From relation (30) it is obvious that, $I_0 = 0$. Now that we have an expression for the, $I_n(\varphi)$, we can rewrite relations (21), (22), (23) and (24). For the internal pseudopotential we get

$$U_{m,int}^{in}(\mathbf{r}) = -\frac{\chi_m^{int}}{2}\sum_{n=1}^{\infty} C_{n,m}\rho^n\left(A_{n,m}\cos(n\varphi) + B_{n,m}\sin(n\varphi)\right) \quad (31)$$

and

$$U_{m,int}^{out}(\mathbf{r}) = -\frac{\chi_m^{int}}{2}\sum_{n=1}^{\infty} C_{n,m}a^{2n}\,\rho^{-n}\left(A_{n,m}\cos(n\varphi) + B_{n,m}\sin(n\varphi)\right) \quad (32)$$

The internal component of the magnetic field gets the form

$$\mathbf{H}_{int}^{in}(\mathbf{r}) = \frac{\chi_m^{int}}{2}\sum_{n=1}^{\infty} C_{n,m}\boldsymbol{\nabla}\left(\rho^n\left(A_{n,m}\cos(n\varphi) + B_{n,m}\sin(n\varphi)\right)\right) \quad (33)$$

for the inside space of the cylinder, $\rho < a$ and

$$\mathbf{H}_{int}^{out}(\mathbf{r}) = \frac{\chi_m^{int}}{2}\sum_{n=1}^{\infty} C_{n,m}a^{2n}\boldsymbol{\nabla}\left(\rho^{-n}\left(A_{n,m}\cos(n\varphi) + B_{n,m}\sin(n\varphi)\right)\right) \quad (34)$$

for the outside space of the cylinder, $\rho > a$.

III.A. Inside space of the magnetic cylinder

Here we provide all details for the case of the inside space. The respective results of the outside space are summarized at the end of this section. As we already stated above, due to the linear

character of the magnetic cylinder, at the inside space the total field is given by relation (25). This means that the general term of the respective expansion, $\mathbf{H}_n^{in}(\mathbf{r})$, gets the form

$$\mathbf{H}_n^{in}(\mathbf{r}) = -C_{n,m}\boldsymbol{\nabla}\left(\rho^n\left(A_{n,m}\cos(n\varphi) + B_{n,m}\sin(n\varphi)\right)\right) \quad (35)$$

Thus, the total field becomes

$$\mathbf{H}^{in}(\mathbf{r}) = -\sum_{n=1}^{\infty} C_{n,m}\boldsymbol{\nabla}\left(\rho^n\left(A_{n,m}\cos(n\varphi) + B_{n,m}\sin(n\varphi)\right)\right) \quad (36)$$

By using the standard constitutive relation $\mathbf{H}^{in}(\mathbf{r}) = -\boldsymbol{\nabla}U_m^{in}(\mathbf{r})$ the respective expression of the total potential at the inside space is given by the relation

$$U_m^{in}(\mathbf{r}) = \sum_{n=0}^{\infty} C_{n,m}\left(\rho^n\left(A_{n,m}\cos(n\varphi) + B_{n,m}\sin(n\varphi)\right)\right) \quad (37)$$

Starting from relation (2) and by using relations (9), (10), (33) and (36) we get

$$-\sum_{n=1}^{\infty} C_{n,m}\boldsymbol{\nabla}U_{m,n,ext}(\mathbf{r}) = -\sum_{n=1}^{\infty}\boldsymbol{\nabla}U_{m,n,ext}(\mathbf{r}) + \sum_{n=1}^{\infty}\frac{\chi_m^{int}}{2}C_{n,m}\boldsymbol{\nabla}U_{m,n,ext}(\mathbf{r}) \quad (38)$$

else

$$\sum_{n=1}^{\infty}\left[C_{n,m}\left(1+\frac{1}{2}\chi_m^{int}\right) - 1\right]\boldsymbol{\nabla}U_{m,n,ext}(\mathbf{r}) = 0 \quad (39)$$

Due to the fact that the vectors $\boldsymbol{\nabla}U_{m,n,ext}(\mathbf{r})$ are linearly independent, the following relation should hold for the respective coefficients

$$C_{n,m}\left(1+\frac{1}{2}\chi_m^{int}\right) - 1 = 0 \quad (40)$$

else

$$C_{n,m} = C_m = \frac{1}{1+\frac{1}{2}\chi_m^{int}} \quad (41)$$

where we have rejected the first subscript, n, since the expansion coefficients do not depend on the order of each mode/term of the external pseudopotential/magnetic field. By defining the depolarization factor

$$N = \frac{1}{2} \quad (42)$$

we finally obtain

$$\mathrm{C_m} = \frac{1}{1 + \mathrm{N}\chi_{\mathrm{m}}^{\mathrm{int}}} \tag{43}$$

Here we should focus on an important finding that clarifies the underlying physics and can be useful in applications. Both the expansion coefficients, $\mathrm{C_{n,m}} = \mathrm{C_m}$, and the depolarization factor, N, are degenerate on the order, n, of the expansion. This means that both $\mathrm{C_m}$ and N attain a constant value irrespectively of the mode, $\mathrm{U_{m,n,ext}}(\mathbf{r})/\mathbf{H}_{\mathrm{n,ext}}(\mathbf{r})$, of the external pseudopotential/field, $\mathrm{U_{m,ext}}(\mathbf{r})/\mathbf{H}_{\mathrm{ext}}(\mathbf{r})$, relations (8) and (10), applied to the magnetic cylinder. In the case of the sphere studied in [36], the respective expansion coefficients exhibited degeneracy on the order, m (however, not on the degree, l) of each mode, $\mathrm{U}^{\mathrm{m}}_{\mathrm{m},l,\mathrm{ext}}(\mathbf{r})/\mathbf{H}^{\mathrm{m}}_{l,\mathrm{ext}}(\mathbf{r})$, of the applied external pseudopotential/field, $\mathrm{U_{m,ext}}(\mathbf{r})/\mathbf{H}_{\mathrm{ext}}(\mathbf{r})$, since $\mathrm{C}_l = 1/\left(1 + \mathrm{N}_l\chi_{\mathrm{e}}^{\mathrm{int}}\right)$. The respective depolarization factor exhibited a similar behavior since $\mathrm{N}_l = l/(2l+1)$.
Returning to the magnetic cylinder studied here, once the expansion coefficients, $\mathrm{C_{n,m}} = \mathrm{C_m}$, have been determined, and given that the expansion coefficients, $\mathrm{A_{n,m}}$ and $\mathrm{B_{n,m}}$ are defined by relations (13) and (13), respectively, the total field of the inside space, relation (36), is given through the following relation

$$\mathbf{H}^{\mathrm{in}}(\mathbf{r}) = -\mathrm{C_m}\sum_{\mathrm{n}=1}^{\infty}\boldsymbol{\nabla}\left(\rho^{\mathrm{n}}\left(\mathrm{A_{n,m}}\cos(\mathrm{n}\varphi) + \mathrm{B_{n,m}}\sin(\mathrm{n}\varphi)\right)\right) \tag{44}$$

Also, using relation (33), we can easily show that the internal field inside the cylinder is given through the following relation

$$\mathbf{H}^{\mathrm{in}}_{\mathrm{int}}(\mathbf{r}) = \sum_{\mathrm{n}=1}^{\infty}\mathbf{H}^{\mathrm{in}}_{\mathrm{n,int}}(\mathbf{r}) = \mathrm{N}\chi_{\mathrm{m}}^{\mathrm{ext}}\sum_{\mathrm{n}=1}^{\infty}\boldsymbol{\nabla}\left(\rho^{\mathrm{n}}\left(\mathrm{A_{n,m}}\cos(\mathrm{n}\varphi) + \mathrm{B_{n,m}}\sin(\mathrm{n}\varphi)\right)\right) \tag{45}$$

where we defined the general term of the expansion and the extrinsic magnetic susceptibility through

$$\mathbf{H}^{\mathrm{in}}_{\mathrm{n,int}}(\mathbf{r}) = \mathrm{N}\chi_{\mathrm{m}}^{\mathrm{ext}}\boldsymbol{\nabla}\left(\rho^{\mathrm{n}}\left(\mathrm{A_{n,m}}\cos(\mathrm{n}\varphi) + \mathrm{B_{n,m}}\sin(\mathrm{n}\varphi)\right)\right) \tag{46}$$

and

$$\chi_{\mathrm{m}}^{\mathrm{ext}} = \frac{\chi_{\mathrm{m}}^{\mathrm{int}}}{1 + \mathrm{N}\chi_{\mathrm{m}}^{\mathrm{int}}} \tag{47}$$

By means of the above definition of coefficient $\mathrm{C_m}$ (relation (43)) and of $\chi_{\mathrm{m}}^{\mathrm{ext}}$ (relation (47)), the total magnetic field inside the magnetic cylinder can be rewritten as following

$$\mathbf{H}^{\mathrm{in}}(\mathbf{r}) = -\frac{\chi_{\mathrm{m}}^{\mathrm{ext}}}{\chi_{\mathrm{m}}^{\mathrm{int}}}\sum_{\mathrm{n}=1}^{\infty}\boldsymbol{\nabla}\left(\rho^{\mathrm{n}}\left(\mathrm{A_{n,m}}\cos(\mathrm{n}\varphi) + \mathrm{B_{n,m}}\sin(\mathrm{n}\varphi)\right)\right) \tag{48}$$

Once we know $\mathbf{H}^{\mathrm{in}}(\mathbf{r})$ the magnetization, $\mathbf{M}(\mathbf{r}) = \chi_{\mathrm{m}}^{\mathrm{int}}\mathbf{H}^{\mathrm{in}}(\mathbf{r})$, of the magnetic cylinder is immediately obtained as following

$$\mathbf{M}(\mathbf{r}) = -\chi_m^{ext} \sum_{n=1}^{\infty} \boldsymbol{\nabla}\left(\rho^n\left(A_{n,m}\cos(n\varphi) + B_{n,m}\sin(n\varphi)\right)\right) \tag{49}$$

Going a step farther, from relations (11) and (46), we can easily obtain the relationship between the general terms of the internal and external fields for the inside space of the cylinder, $\rho < a$, as following

$$\mathbf{H}_{n,int}^{in}(\mathbf{r}) = -N\chi_m^{ext}\mathbf{H}_{n,ext}^{in}(\mathbf{r}) \tag{50}$$

This relation is quite useful for applications. It defines the response of the magnetic cylinder to the external cause. Also, by using relation (47), we see that the prefactor of the right side is, also, written as following

$$N\chi_m^{ext} = \frac{N\chi_m^{int}}{1 + N\chi_m^{int}} \tag{51}$$

By defining the effective intrinsic magnetic susceptibility through

$$\chi_m^N = N\chi_m^{int} \tag{52}$$

Thus, the above relation (50) is rewritten as following

$$\mathbf{H}_{n,int}^{in}(\mathbf{r}) = -\frac{\chi_m^N}{1 + \chi_m^N}\mathbf{H}_{n,ext}^{in}(\mathbf{r}) \tag{53}$$

Finally, to facilitate their applicability, below we summarize the relations of the internal and total pseudopotentials for the inside space of the magnetic cylinder, as following

$$U_{m,int}^{in}(\mathbf{r}) = \sum_{n=0}^{\infty} U_{m,n,int}^{in}(\mathbf{r}) = -N\chi_m^{ext}\sum_{n=0}^{\infty}\rho^n\left(A_{n,m}\cos(n\varphi) + B_{n,m}\sin(n\varphi)\right) \tag{54}$$

and

$$U_m^{in}(\mathbf{r}) = \sum_{n=0}^{\infty} U_{m,n}^{in}(\mathbf{r}) = C_m\sum_{n=0}^{\infty}\rho^n\left(A_{n,m}\cos(n\varphi) + B_{n,m}\sin(n\varphi)\right) \tag{55}$$

where we defined the relevant general term of each expansion through

$$U_{m,n,int}^{in}(\mathbf{r}) = -N\chi_m^{ext}\rho^n\left(A_{n,m}\cos(n\varphi) + B_{n,m}\sin(n\varphi)\right) \tag{56}$$

and

$$U_n^{in}(\mathbf{r}) = C_m\rho^n\left(A_{n,m}\cos(n\varphi) + B_{n,m}\sin(n\varphi)\right) \tag{57}$$

Accordingly, we easily see that the general terms of the internal and external pseudopotentials follow the relation

$$U^{in}_{m,n,int}(\mathbf{r}) = -N\chi^{ext}_m U^{in}_{m,n,ext}(\mathbf{r}) = -\frac{\chi^N_m}{1+\chi^N_m} U^{in}_{m,n,ext}(\mathbf{r}) \quad (58)$$

III.B. Outside space of the magnetic cylinder

The results for the outside space of the magnetic cylinder are summarized here, without any details on the algebraic calculations. We note that the external pseudopotential/field, $U_{m,ext}(\mathbf{r})/\mathbf{H}_{ext}(\mathbf{r})$, are given by the same relations (8) and (10), as for the inside space of the cylinder. By using the same algebraic approach described above we obtain the following results

$$\mathbf{H}^{out}_{int}(\mathbf{r}) = \sum_{n=1}^{\infty} \mathbf{H}^{out}_{n,int}(\mathbf{r}) = N\chi^{ext}_m \sum_{n=1}^{\infty} a^{2n} \nabla\left(\rho^{-n}\left(A_{n,m}\cos(n\varphi) + B_{n,m}\sin(n\varphi)\right)\right) \quad (59)$$

for the internal magnetic field, and

$$\mathbf{H}^{out}(\mathbf{r}) = -\sum_{n=1}^{\infty} \nabla\left(\rho^{n}\left(A_{n,m}\cos(n\varphi) + B_{n,m}\sin(n\varphi)\right)\right) + N\chi^{ext}_m \sum_{n=1}^{\infty} a^{2n} \nabla\left(\rho^{-n}\left(A_{n,m}\cos(n\varphi) + B_{n,m}\sin(n\varphi)\right)\right) \quad (60)$$

for the total magnetic field. The respective relations for the internal and total magnetic pseudopotential are the following

$$U^{out}_{m,int}(\mathbf{r}) = \sum_{n=0}^{\infty} U^{out}_{m,n,int}(\mathbf{r}) = -N\chi^{ext}_m \sum_{n=0}^{\infty} \frac{a^{2n}}{\rho^n}\left(A_{n,m}\cos(n\varphi) + B_{n,m}\sin(n\varphi)\right) \quad (61)$$

and

$$U^{out}_{m}(\mathbf{r}) = \sum_{n=0}^{\infty} \rho^n\left(A_{n,m}\cos(n\varphi) + B_{n,m}\sin(n\varphi)\right) - N\chi^{ext}_m \sum_{n=0}^{\infty} \frac{a^{2n}}{\rho^n}\left(A_{n,m}\cos(n\varphi) + B_{n,m}\sin(n\varphi)\right) \quad (62)$$

Obviously, the obtained results hold for the case where the external magnetic field, $\mathbf{H}_{ext}(\mathbf{r})$, is either DC (static case) or AC, time-harmonic of low-frequency (quasistatic case), e.g. the spatially-homogeneous $\mathbf{H}_{ext}(\mathbf{r}) = \mathbf{H}_0\cos(\omega t)$. Thus, these results can be utilized in many applications of magnetic cylinders.

IV. Dielectric cylinder -linear, homogeneous and isotropic- subjected to an external scalar potential/vector field of *any* form

In this section we summarize the respective relations that hold for the relevant case of the dielectric cylinder of radius a, which constitutes of linear, homogeneous and isotropic material of

intrinsic susceptibility χ_e^{int}, when subjected to an external potential/field, $U_{ext}(\mathbf{r})/\mathbf{E}_{ext}(\mathbf{r})$. These are produced by a primary source (e.g. free electric charges) that resides outside the dielectric cylinder. The secondary source of bound charges that resides at the surface of the dielectric cylinder, due to the discontinuity of the polarization, $\mathbf{P}(\mathbf{r})$, will produce the internal $U_{int}(\mathbf{r})/\mathbf{E}_{int}(\mathbf{r})$. The total $U(\mathbf{r})/\mathbf{E}(\mathbf{r})$ are provided by

$$U(\mathbf{r}) = U_{ext}(\mathbf{r}) + U_{int}(\mathbf{r}) \tag{63}$$

and

$$\mathbf{E}(\mathbf{r}) = \mathbf{E}_{ext}(\mathbf{r}) + \mathbf{E}_{int}(\mathbf{r}) \tag{64}$$

Again, we refer to the most general case where the external $U_{ext}(\mathbf{r})/\mathbf{E}_{ext}(\mathbf{r})$ can be of *any* form. Thus, $U_{ext}(\mathbf{r})$ is expanded as following

$$U_{ext}(\mathbf{r}) = \sum_{n=0}^{\infty} U_{n,ext}(\mathbf{r}) = A_0 + \sum_{n=1}^{\infty} \rho^n (A_n \cos(n\varphi) + B_n \sin(n\varphi)) \tag{65}$$

The general term of the expansion is defined as following

$$U_{n,ext}(\mathbf{r}) = \rho^n (A_n \cos(n\varphi) + B_n \sin(n\varphi)) \tag{66}$$

The necessary expansion coefficients, A_n and B_n, are given through the following relations

$$A_0 = \frac{1}{2\pi} \int_0^{2\pi} U_{ext}(\mathbf{r}) d\varphi \tag{67}$$

$$A_n = \frac{1}{\pi \rho^n} \int_0^{2\pi} U_{ext}(\mathbf{r}) \cos(n\varphi)\, d\varphi \tag{68}$$

$$B_n = \frac{1}{\pi \rho^n} \int_0^{2\pi} U_{ext}(\mathbf{r}) \sin(n\varphi)\, d\varphi \tag{69}$$

Similarly, $\mathbf{E}_{ext}(\mathbf{r})$, due to the constitutive relation $\mathbf{E}_{ext}(\mathbf{r}) = -\boldsymbol{\nabla} U_{ext}(\mathbf{r})$, should follow the respective expansion

$$\mathbf{E}_{ext}(\mathbf{r}) = \sum_{n=1}^{\infty} \mathbf{E}_{n,ext}(\mathbf{r}) = -\sum_{n=1}^{\infty} \boldsymbol{\nabla}\left(\rho^n (A_n \cos(n\varphi) + B_n \sin(n\varphi))\right) \tag{70}$$

The general term of the expansion is defined as following

$$\mathbf{E}_{n,ext}(\mathbf{r}) = -\boldsymbol{\nabla}\left(\rho^n (A_n \cos(n\varphi) + B_n \sin(n\varphi))\right) \tag{71}$$

The above expressions of the external $U_{ext}(\mathbf{r})/\mathbf{E}_{ext}(\mathbf{r})$ hold throughout the whole space, that is for both the inside and outside space of the dielectric cylinder. Now that we have at hand the necessary information for the external potential/field, we can summarize the relations for the respective internal, $U_{int}(\mathbf{r})/\mathbf{E}_{int}(\mathbf{r})$, and total, $U(\mathbf{r})/\mathbf{E}(\mathbf{r})$, components, also, for both the inside and outside space of the cylinder. This is done below.

IV.A. Inside space of the dielectric cylinder

For $\rho \leq a$ the internal electric field is given by the following relation

$$\mathbf{E}_{int}^{in}(\mathbf{r}) = \sum_{n=0}^{\infty} \mathbf{E}_{n,int}^{in}(\mathbf{r}) = N\chi_e^{ext} \sum_{n=1}^{\infty} \boldsymbol{\nabla}\left(\rho^n (A_n \cos(n\varphi) + B_n \sin(n\varphi))\right) \tag{72}$$

The general term of the expansion is given by the relation

$$\mathbf{E}_{n,int}^{in}(\mathbf{r}) = N\chi_e^{ext} \boldsymbol{\nabla}\left(\rho^n (A_n \cos(n\varphi) + B_n \sin(n\varphi))\right) \tag{73}$$

The extrinsic electric susceptibility is provided through the relation

$$\chi_e^{ext} = \frac{\chi_e^{int}}{1 + N\chi_e^{int}} \tag{74}$$

The total electric field inside the cylinder is given through the relation

$$\mathbf{E}^{in}(\mathbf{r}) = -C \sum_{n=1}^{\infty} \boldsymbol{\nabla}\left(\rho^n (A_n \cos(n\varphi) + B_n \sin(n\varphi))\right) \tag{75}$$

where the coefficients, C_n, are given by the relation

$$C_n = C = \frac{1}{1 + \frac{1}{2}\chi_e^{int}} = \frac{1}{1 + N\chi_e^{int}} \tag{76}$$

The total electric field obtains the following form

$$\mathbf{E}^{in}(\mathbf{r}) = -\frac{\chi_e^{ext}}{\chi_e^{int}} \sum_{n=1}^{\infty} \boldsymbol{\nabla}\left(\rho^n (A_n \cos(n\varphi) + B_n \sin(n\varphi))\right) \tag{77}$$

The relation between the general terms of the internal and external electric fields is the following

$$\mathbf{E}_{n,int}^{in}(\mathbf{r}) = -N\chi_e^{ext} \mathbf{E}_{n,ext}^{in}(\mathbf{r}) \tag{78}$$

By defining

$$N\chi_e^{ext} = \frac{N\chi_e^{int}}{1 + N\chi_e^{int}} \tag{79}$$

and the effective intrinsic electric susceptibility through

$$\chi_e^N = N\chi_e^{int} \tag{80}$$

we get the equivalent relation

$$\mathbf{E}_{n,int}^{in}(\mathbf{r}) = -\frac{\chi_e^N}{1 + \chi_e^N}\mathbf{E}_{n,ext}^{in}(\mathbf{r}) \tag{81}$$

The polarization $\mathbf{P}(\mathbf{r}) = \varepsilon_0\chi_e^{int}\mathbf{E}^{in}(\mathbf{r})$ is given by the following relation

$$\mathbf{P}(\mathbf{r}) = -\varepsilon_0\chi_e^{ext}\sum_{n=1}^{\infty}\nabla\left(\rho^n(A_n\cos(n\varphi) + B_n\sin(n\varphi))\right) \tag{82}$$

The relations of the internal and total potentials for the inside space of the dielectric cylinder are as followings

$$U_{int}^{in}(\mathbf{r}) = \sum_{n=0}^{\infty}U_{n,int}^{in}(\mathbf{r}) = -N\chi_e^{ext}\sum_{n=0}^{\infty}\rho^n(A_n\cos(n\varphi) + B_n\sin(n\varphi)) \tag{83}$$

and

$$U^{in}(\mathbf{r}) = \sum_{n=0}^{\infty}U_n^{in}(\mathbf{r}) = C\sum_{n=0}^{\infty}\rho^n(A_n\cos(n\varphi) + B_n\sin(n\varphi)) \tag{84}$$

where we defined the relevant general term of each expansion as following

$$U_{n,int}^{in}(\mathbf{r}) = -N\chi_e^{ext}\rho^n(A_n\cos(n\varphi) + B_n\sin(n\varphi)) \tag{85}$$

and

$$U_n^{in}(\mathbf{r}) = C\rho^n(A_n\cos(n\varphi) + B_n\sin(n\varphi)) \tag{86}$$

The general terms of the internal and external potentials relate through

$$U_{n,int}^{in}(\mathbf{r}) = -N\chi_e^{ext}U_{n,ext}^{in}(\mathbf{r}) \tag{87}$$

IV.B. Outside space of the dielectric cylinder

For $\rho \geq a$ the internal electric field is given by the following relation

$$\mathbf{E}_{\text{int}}^{\text{out}}(\mathbf{r}) = \sum_{n=1}^{\infty} \mathbf{E}_{n,\text{int}}^{\text{out}}(\mathbf{r}) = N\chi_e^{\text{ext}} \sum_{n=1}^{\infty} a^{2n} \boldsymbol{\nabla}\left(\rho^{-n}(A_n \cos(n\varphi) + B_n \sin(n\varphi))\right) \quad (88)$$

The total electric field inside the cylinder is given through the relation

$$\mathbf{E}^{\text{out}}(\mathbf{r}) = -\sum_{n=1}^{\infty} \boldsymbol{\nabla}\left(\rho^{n}(A_n \cos(n\varphi) + B_n \sin(n\varphi))\right) + N\chi_e^{\text{ext}} \sum_{n=1}^{\infty} a^{2n} \boldsymbol{\nabla}\left(\rho^{-n}(A_n \cos(n\varphi) + B_n \sin(n\varphi))\right) \quad (89)$$

The respective relations for the internal, $U_{\text{int}}^{\text{out}}(\mathbf{r})$, and total, $U^{\text{out}}(\mathbf{r})$, potentials for $\rho \geq a$ are the followings

$$U_{\text{int}}^{\text{out}}(\mathbf{r}) = \sum_{n=0}^{\infty} U_{n,\text{int}}^{\text{out}}(\mathbf{r}) = -N\chi_e^{\text{ext}} \sum_{n=0}^{\infty} \frac{a^{2n}}{\rho^n}(A_n \cos(n\varphi) + B_n \sin(n\varphi)) \quad (90)$$

and

$$U^{\text{out}}(\mathbf{r}) = \sum_{n=0}^{\infty} \rho^n(A_n \cos(n\varphi) + B_n \sin(n\varphi)) - N\chi_e^{\text{ext}} \sum_{n=0}^{\infty} \frac{a^{2n}}{\rho^n}(A_n \cos(n\varphi) + B_n \sin(n\varphi)) \quad (91)$$

Again, these results hold for the case where $\mathbf{E}_{\text{ext}}(\mathbf{r})$ is either a DC field (static case) or a time-harmonic AC field, however, of low frequency (quasistatic case), e.g. $\mathbf{E}_{\text{ext}}(\mathbf{r}) = \mathbf{E}_0 \cos(\omega t)$. Thus, these results can be useful in many applications of dielectric cylinders.

V. Summary of our findings and utilization in applications

The above extended mathematical part needs a summary to facilitate its understanding and applicability. To this effect, two representative applications are briefly discussed below, one for a magnetic and one for a dielectric cylinder subjected to a field that from a mathematical point of view is quite demanding.

V.A. Summary of our findings

First of all, we recall that our method is based on the expansion of the external pseudopotential/field, $U_{m,\text{ext}}(\mathbf{r})/\mathbf{H}_{\text{ext}}(\mathbf{r})$, on the basis of the particular space. To this end, relations (8)-(9) and (10)-(11), are needed, while the respective expansion coefficients, $A_{n,m}$ and $B_{n,m}$, are available through relations (12), (13) and (14). Notably, these relations hold for the entire space, that is both inside and outside the magnetic cylinder. Referring to the inside space, the internal and total pseudopotentials, $U_{m,\text{int}}^{\text{in}}(\mathbf{r})$ and $U_{m}^{\text{in}}(\mathbf{r})$, are given through relations (54) and (55), respectively, while $U_{m,\text{int}}^{\text{in}}(\mathbf{r})$ and $U_{m,\text{ext}}^{\text{in}}(\mathbf{r})$ relate through relation (58). The respective internal and total fields, $\mathbf{H}_{\text{int}}^{\text{in}}(\mathbf{r})$ and $\mathbf{H}^{\text{in}}(\mathbf{r})$, are given through relations (45) and (48), respectively, while $\mathbf{H}_{\text{int}}^{\text{in}}(\mathbf{r})$ and $\mathbf{H}_{\text{ext}}^{\text{in}}(\mathbf{r})$ relate through relations (50) and (53). For the outside

space, relations (61)-(**Error! Reference source not found.**) and (59)-(60), hold for the internal and total pseudopotentials, $U_{m,int}^{out}(\mathbf{r})$ and $U_{m}^{out}(\mathbf{r})$, and fields, $\mathbf{H}_{int}^{out}(\mathbf{r})$ and $\mathbf{H}^{out}(\mathbf{r})$, respectively. All above relations are useful when the following ingredients are known: the expansion coefficients, C_m (relation (43)), the demagnetizing factor, N (relation (42)) and the extrinsic magnetic susceptibility, χ_m^{ext} (relation (47)). Finally, the magnetization, $\mathbf{M}(\mathbf{r})$, of the magnetic cylinder is given through relation (49). The respective relations for the case of a dielectric cylinder are provided in section III for the external potential/field, in section III.1 for the internal and total potential/field of the inside space, and in section III.2 for the internal and total potential/field of the outside space. The polarization, $\mathbf{P}(\mathbf{r})$, of the dielectric cylinder is given through relation (82).

The universal expressions derived above hold for any form of the external potential/field. Their profound advantage is that they are ready-to-use, thus providing the necessary solutions for all, internal and total potentials and fields, and the polarization, in practically one step. Thus, there is no need to solve each different problem from the beginning through the application of lengthy algebraic calculations.

To efficiently use these universal expressions the following procedure should be followed. First, the non-zero expansion coefficients and non-null modes n of the external pseudopotential/field should be found. These refer to $A_{n,m}$, $B_{n,m}$ for the magnetic and A_n, B_n for the electric case, that can be obtained through relations (12), (13), (14) and (67), (68), (69) respectively. Second, the expansion coefficients, C_m for the magnetic and C for the dielectric case, are immediately calculated through relations (43) and (76), respectively. Then, both the internal and total pseudopotentials/fields are easily calculated everywhere in space, that is both inside and outside the cylinder, as summarized above. Also, the polarization is calculated for the inside space of the cylinder. Finally, referring to the fields, the vector functions $\boldsymbol{\nabla}(\rho^n \cos(n\varphi))$, $\boldsymbol{\nabla}(\rho^n \sin(n\varphi))$, $\boldsymbol{\nabla}(\rho^{-n} \cos(n\varphi))$ and $\boldsymbol{\nabla}(\rho^{-n} \sin(n\varphi))$ are needed for the non-null modes n of every problem. Obviously, there is no need to calculate these functions from scratch every time we have to address a new problem. Tables of these functions are easily constructed for general use. For instance, for the case of the dielectric and magnetic sphere the respective functions $\boldsymbol{\nabla}(r^l Y_l^m(\theta,\varphi))$ and $\boldsymbol{\nabla}(r^{-(l+1)} Y_l^m(\theta,\varphi))$ are needed. The first ones, for degree up to $l = 2$, can be found in the Table of Appendix B in [36]. Such Tables can be easily set up for the case of dielectric and magnetic cylinder as well, to minimize the algebraic effort. Finally, the analytical form of the universal expressions presented here for cylinders and in [36] for spheres, sets a reliable and convenient basis for computational studies, to minimize requirements on resources.

V.B. Utilization of our findings in applications

To document the advantages of our universal expressions, here we address two rather demanding cases, one for a magnetic and one for a dielectric cylinder. The eager reader is invited to use standard approaches of electromagnetism, that unavoidably go through time-consuming algebraic calculations, to check the validity of the results provided below in these two representative problems. Immediately, becomes apparent that our approach provides the exact same results, reliably and effortlessly.

V.B.1. First case: A linear, homogeneous and isotropic magnetic cylinder of radius, a and intrinsic susceptibility, χ_m^{int}, with its axis coinciding with the z axis. The cylinder is subjected to an external pseudopotential, $U_{m,ext}(\mathbf{r})$, produced by two infinitely long wires, parallel to the z axis placed at $x = -b$, and $x = b$ ($a < b$). The wires carry a current of $\mathbf{I}(x = -b) = -I_0\hat{\mathbf{z}}$ and

$\mathbf{I}(x = b) = I_0\hat{\mathbf{z}}$ (see problem 5.15, page 228 in [33]). This configuration creates the following external pseudopotential [33]

$$U_{m,ext}(\mathbf{r}) = \frac{I_0}{2\pi}\left(\arctan\left[\frac{\rho\sin\varphi}{b-\rho\cos\varphi}\right] + \arctan\left[\frac{\rho\sin\varphi}{b+\rho\cos\varphi}\right]\right) \quad (92)$$

By using relations (12), (13) and (14) we obtain the expansion coefficients

$$A_{n,m} = 0, \quad \text{for every n} \quad (93)$$
$$B_{n,m} = 0, \quad \text{n even} \quad (94)$$
$$B_{n,m} = \frac{I_0}{\pi}\frac{1}{b^n}, \quad \text{n odd} \quad (95)$$

Thus, the external pseudopotential, using relation (8), can be rewritten as

$$U_{m,ext}(\mathbf{r}) = \frac{I_0}{\pi}\sum_{n\ odd}^{\infty}\left(\frac{\rho}{b}\right)^n \sin(n\varphi) \quad (96)$$

This relation of $U_{m,ext}(\mathbf{r})$ holds for both the inside and outside spaces, that is $U_{m,ext}(\mathbf{r}) = U^{in}_{m,ext}(\mathbf{r}) = U^{out}_{m,ext}(\mathbf{r})$. Substituting this information into the appropriate relations we can obtain the internal and total pseudopotentials and fields, for both the inside and outside space of the magnetic cylinder as following.

Inside space: By substituting relations (93), (94) and (95) into relation (54) we obtain the internal pseudopotential

$$U^{in}_{m,int}(\mathbf{r}) = -N\chi^{ext}_m\frac{I_0}{\pi}\sum_{n\ odd}^{\infty}\left(\frac{\rho}{b}\right)^n \sin(n\varphi) = -N\chi^{ext}_m U^{in}_{m,ext}(\mathbf{r}) \quad (97)$$

Also, by simply substituting relation (97) into relation (55) we obtain the total pseudopotential

$$U^{in}_{m}(\mathbf{r}) = \frac{\chi^{ext}_m}{\chi^{int}_m}\frac{I_0}{\pi}\sum_{n\ odd}^{\infty}\left(\frac{\rho}{b}\right)^n \sin(n\varphi) = \frac{\chi^{ext}_m}{\chi^{int}_m}U^{in}_{m,ext}(\mathbf{r}) \quad (98)$$

It can be easily verified that the above result is absolutely the same with the one that is obtained with the standard, time-consuming mathematical approach that is based on step-by-step solution of the problem.

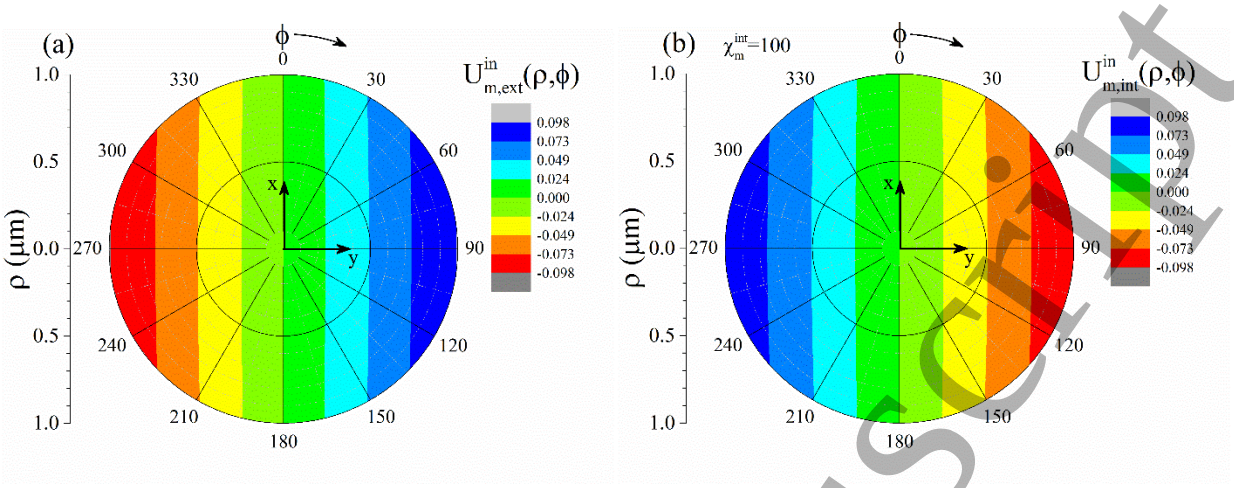

Figure 4. Simulations of relations (96) and (97) (the first five terms with $n = 1, 3, 5, 7$ and 9 are considered) via polar plots of the (a) external, $U^{in}_{m,ext}(\mathbf{r})$,and the (b) internal, $U^{in}_{m,int}(\mathbf{r})$, pseudopotentials at the inside space, $\rho \leq a$, for a linear, homogeneous and isotropic magnetic cylinder with $a = 1$ μm, depolarization factor, $N = 1/2$, and intrinsic susceptibility, $\chi_m^{int} = 100$. The coaxial-to-z source wires are characterized by $\mathbf{I}(x = \pm 10\ \mu m) = \pm I_0 \hat{\mathbf{z}}$ with $I_0 = 3.14$ A. The color bars refer to the intensity of the pseudopotentials and are exactly the same for the two panels.

Figures 4(a)-4(b) present simulations for the inside space of the cylinder, $\rho \leq a$, for realistic parameters. Specifically, we present polar plots of the pseudopotentials, the external, $U^{in}_{m,ext}(\mathbf{r})$ (panel (a)), applied by the primary free source, and the internal, $U^{in}_{m,int}(\mathbf{r})$ (panel (b)), as produced by the secondary bound source. The magnetic cylinder is linear, homogeneous and isotropic with radius, $a = 1$ μm, depolarization factor, $N = 1/2$ and intrinsic susceptibility, $\chi_m^{int} = 100$. It should be noted that the particular value of χ_m^{int} is absolutely realistic (being rather low), exhibited by many typical magnetic materials. The two wires placed at $x = \pm 10$ μm provide the free sources of the DC currents $\mathbf{I}(x = \pm 10\ \mu m) = \pm I_0 \hat{\mathbf{z}}$, with a value $I_0 = 3.14$ A. Panel (a) simulates relation (96), while panel (b) simulates relation (97). From these simulations becomes evident that $U^{in}_{m,ext}(\mathbf{r})$ and $U^{in}_{m,int}(\mathbf{r})$ are mirror images in respect to the xz-plane. Notice that the color bars of the two panels have the exact same range. Thus, the particular cylinder responds with an internal $U^{in}_{m,int}(\mathbf{r})$ that practically cancels the applied external $U^{in}_{m,ext}(\mathbf{r})$, that is $U^{in}_{m,int}(\mathbf{r}) \approx -U^{in}_{m,ext}(\mathbf{r})$, leading to completely shielding of its inside space. Obviously, the same holds for the respective magnetic field.

Outside space: By substituting relations (93), (94) and (95) into relation (61) we obtain the internal pseudopotential

$$U^{out}_{m,int}(\mathbf{r}) = -N\chi_m^{ext}\frac{I_0}{\pi}\sum_{n\ odd}^{\infty}\left(\frac{a}{\rho}\right)^{2n}\left(\frac{\rho}{b}\right)^{n}\sin(n\varphi) \qquad (99)$$

while by using relation (**Error! Reference source not found.**) we obtain the total pseudopotential

$$U_m^{out}(\mathbf{r}) = \frac{I_0}{\pi}\sum_{n\ odd}^{\infty}\left(1 - N\chi_m^{ext}\left(\frac{a}{\rho}\right)^{2n}\right)\left(\frac{\rho}{b}\right)^{n}\sin(n\varphi) \quad (100)$$

Again, it can be easily verified that the above result is in nice agreement with that of the standard, time-consuming mathematical approach. By using the respective relations for the internal and total magnetic fields we can find these entities both inside, $\mathbf{H}_{int}^{in}(\mathbf{r})$ and $\mathbf{H}^{in}(\mathbf{r})$, and outside, $\mathbf{H}_{int}^{out}(\mathbf{r})$ and $\mathbf{H}^{out}(\mathbf{r})$, the magnetic cylinder.

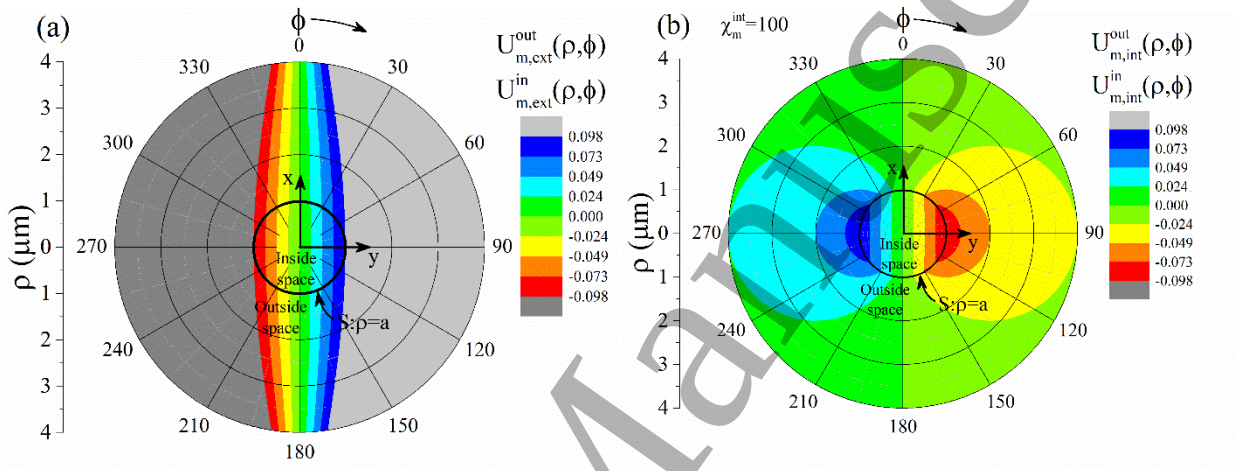

Figure 5. Simulations of relations (96) and (99) (the first five terms with $n = 1, 3, 5, 7$ and 9 are considered) via polar plots of the (a) external, $U_{m,ext}^{out}(\mathbf{r})$, and (b) internal, $U_{m,int}^{out}(\mathbf{r})$, pseudopotentials at the outside space, $a \leq \rho$, for the same parameters of Figure 4. The respective data of the inside space, $U_{m,ext}^{in}(\mathbf{r})$ and $U_{m,int}^{in}(\mathbf{r})$, are, also, presented. The color bars refer to the intensity of the pseudopotentials and are exactly the same for the two panels.

Figures 5(a)-5(b) present the respective polar plots of the external, $U_{m,ext}^{out}(\mathbf{r})$ (panel (a)) and the internal, $U_{m,int}^{out}(\mathbf{r})$ (panel (b)) for the outside space, $a \leq \rho$. Notice that in both panels we have focused on the same range of the color bars. The respective data of the inside space, $U_{m,ext}^{in}(\mathbf{r})$ and $U_{m,int}^{in}(\mathbf{r})$, are, also, included to document the continuity of both pseudopotentials at the interface, $\rho = a$, as expected. Accordingly, panel (a) simulates relation (96), while panel (b) simulates relation (99). From these simulations becomes evident that the response of the magnetic cylinder $U_{m,int}^{in}(\mathbf{r})$ exhibits a robust dipolar character in the outside space. Indeed, this is confirmed by relation (97) where, evidently, the dependence on the radial variable attains the same form ρ^{-2}, irrespectively of the value of n. Unfortunately, the degenerate character of the depolarization factor, $N = 1/2$, does not leave much space for engineering the response, $U_{m,int}^{out}(\mathbf{r})$, of the magnetic cylinder in respect to the specific form of the applied external pseudopotential, $U_{m,ext}^{out}(\mathbf{r})$.

V.B.2. Second case: A linear, homogeneous and isotropic dielectric cylinder of radius, a and intrinsic susceptibility, χ_e^{int}, with its axis coinciding with the z axis. The cylinder is subjected to an external potential, $U_{ext}(\mathbf{r})$, produced by a coaxial, thickless cylindrical shell of radius, b ($a <$

b). The cylindrical shell carries the primary source, a surface density of free charge, $\sigma_f(b,\varphi) = \sigma_0 \cos(m\varphi)$, which creates the following external potential

$$U_{ext}(\mathbf{r}) = \frac{E_0}{2m}\frac{\rho^m}{b^{m-1}}\cos(m\varphi) \tag{101}$$

where, $E_0 = \sigma_0/\varepsilon_0$, while $m = 1,2,3,\ldots,\infty$. This relation of $U_{ext}(\mathbf{r})$ holds for both the inside and outside spaces, that is $U_{ext}(\mathbf{r}) = U_{ext}^{in}(\mathbf{r}) = U_{ext}^{out}(\mathbf{r})$. By using relations (67), (68) and (69) we obtain the expansion coefficients

$$A_n = 0, \quad n \neq m \tag{102}$$

$$A_n = \frac{E_0}{2nb^{n-1}}, \quad n = m \tag{103}$$

$$B_n = 0, \quad \text{for every } n \tag{104}$$

Substituting this information into the appropriate relations we can obtain the internal and total potentials and fields, for both the inside and outside space of the dielectric cylinder as following.
Inside space: By substituting relations (102), (103) and (104) into relation (83) we obtain the internal potential

$$U_{int}^{in}(\mathbf{r}) = -N\chi_e^{ext}\frac{E_0}{2n}\frac{\rho^n}{b^{n-1}}\cos(n\varphi) = -N\chi_e^{ext}U_{ext}^{in}(\mathbf{r}) \tag{105}$$

Also, by simply substituting relation (105) into relation (86) we obtain the total potential

$$U^{in}(\mathbf{r}) = \frac{\chi_e^{ext}}{\chi_e^{int}}\frac{E_0}{2n}\frac{\rho^n}{b^{n-1}}\cos(n\varphi) = \frac{\chi_e^{ext}}{\chi_e^{int}}U_{ext}^{in}(\mathbf{r}) \tag{106}$$

It can be easily verified that the above result agrees with that obtained with the standard, time-consuming mathematical approach.

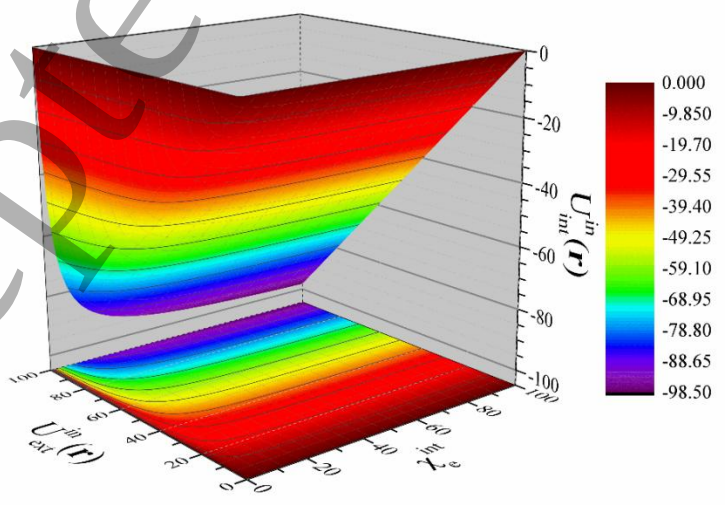

Figure 6. Simulations of relation (105), that is of the internal potential, $U_{int}^{in}(\mathbf{r})$, as function of the external potential, $U_{ext}^{in}(\mathbf{r})$, and intrinsic susceptibility, χ_e^{int}, at the inside space, $\rho \leq a$. The color bar refers to the intensity of $U_{int}^{in}(\mathbf{r})$.

Outside space: By substituting relations (102), (103) and (104) into relation (90) we obtain the internal potential

$$U_{int}^{out}(\mathbf{r}) = -N\chi_e^{ext}\left(\frac{a}{\rho}\right)^{2n}\frac{E_0}{2n}\frac{\rho^n}{b^{n-1}}\cos(n\varphi) = -N\chi_e^{ext}\left(\frac{a}{\rho}\right)^{2n}U_{ext}^{out}(\mathbf{r}) \tag{107}$$

while by using relation (**Error! Reference source not found.**) we obtain the total potential

$$U^{out}(\mathbf{r}) = \left(1 - N\chi_e^{ext}\left(\frac{a}{\rho}\right)^{2n}\right)\frac{E_0}{2n}\frac{\rho^n}{b^{n-1}}\cos(n\varphi) \tag{108}$$

Again, it can be easily verified that the above result agrees with that obtained with the standard, time-consuming mathematical approach. By using the respective relations for the internal and total electric fields we can find these entities both inside, $\mathbf{E}_{int}^{in}(\mathbf{r})$ and $\mathbf{E}^{in}(\mathbf{r})$, and outside, $\mathbf{E}_{int}^{out}(\mathbf{r})$ and $\mathbf{E}^{out}(\mathbf{r})$, the dielectric cylinder.

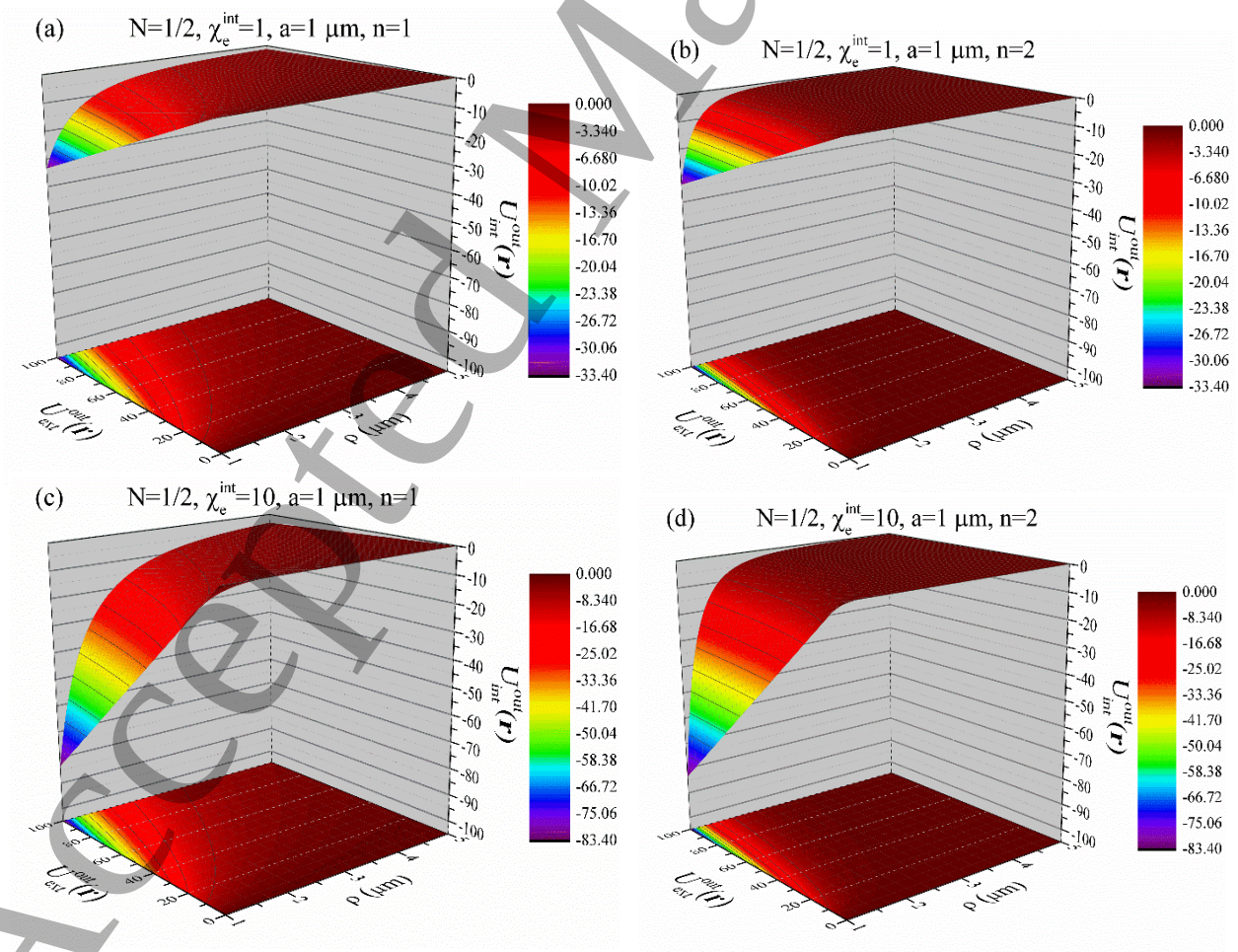

Figure 7. Simulations of relation (90), that is of the internal potential, $U_{int}^{out}(\mathbf{r})$, as function of the external potential, $U_{ext}^{out}(\mathbf{r})$, and intrinsic susceptibility, χ_e^{int}, at the outside space, $a = 1\ \mu m \leq \rho \leq 5\ \mu m$, for realistic values of the involved parameters. The radius of the charged cylindrical shell that produces the external potential is $b = 10\ \mu m$ (see text for details). The depolarization factor, N, and the radius, a, attain the same value in all four cases, $N = 1/2$ and $a = 1\ \mu m$. (a) Intrinsic susceptibility, $\chi_e^{int} = 1$, and order of external potential, $n = 1$. (b) Intrinsic susceptibility, $\chi_e^{int} = 1$, and order of external potential, $n = 2$. (c) Intrinsic susceptibility, $\chi_e^{int} = 10$, and order of external potential, $n = 1$. (d) Intrinsic susceptibility, $\chi_e^{int} = 10$, and order of external potential, $n = 2$. In all panels, the color bars refer to the intensity of $U_{int}^{out}(\mathbf{r})$.

Figures 7(a)-7(d) present detailed simulations of relation (90), that is of the internal potential, $U_{int}^{out}(\mathbf{r})$, in respect to the applied external potential, $U_{ext}^{out}(\mathbf{r})$, and intrinsic susceptibility, χ_e^{int}, for the outside space, $a \leq \rho$. Realistic values are employed for all involved parameters. In all four cases the depolarization factor, N, and the radius, a, of the dielectric cylinder attain the same value, $N = 1/2$ and $a = 1\ \mu m$, while the intrinsic susceptibility, χ_e^{int}, and the order of external potential, n, differ from panel to panel.

Panel (a) refers to $\chi_e^{int} = 1$ and $n = 1$. We see that due to the relatively low value of χ_e^{int} the cylinder cannot shield its outside space effectively from the applied external potential. Thus, for the maximum value of $U_{ext}^{out}(\mathbf{r}) = 100\ V$, the internal potential attains the maximum screening value $U_{int}^{out}(\mathbf{r}) = -33.40\ V$ at the interface, $\rho = a = 1\ \mu m$. As we move radially, away from the cylinder-vacuum interface, the screening efficiency drops rapidly, since $U_{int}^{out}(\mathbf{r})$ attains an absolute value below 10% of $U_{ext}^{out}(\mathbf{r})$ just within 1 μm, that is for $a = 1\ \mu m \leq \rho \leq 2\ \mu m$. Panel (b) refers to $\chi_e^{int} = 1$ and $n = 2$. Again, we see that for the maximum value of $U_{ext}^{out}(\mathbf{r}) = 100\ V$, the internal potential attains the maximum screening value $U_{int}^{out}(\mathbf{r}) = -33.40\ V$ at the interface, $\rho = a = 1\ \mu m$. However, due to the higher value of the order, n, of the external potential, $U_{ext}^{out}(\mathbf{r})$, the term $(a/\rho)^{2n}$ now exerts a stronger influence on the internal potential, $U_{int}^{out}(\mathbf{r})$ (see relation 107), so that it drops off even more rapidly in comparison to the first case. Thus, at a distance 1 μm from the cylinder-vacuum interface $U_{int}^{out}(\mathbf{r})$ attains an absolute value below 5% of $U_{ext}^{out}(\mathbf{r})$. Panels (c) and (d) refer both to $\chi_e^{int} = 10$, while the order, n, of $U_{ext}^{out}(\mathbf{r})$ is $n = 1$ and $n = 2$, respectively. We see that due to the significantly higher value of χ_e^{int} the cylinder now shields its outside space close effectively from the applied external potential, at least at its close neighborhood. Specifically, for the maximum value of $U_{ext}^{out}(\mathbf{r}) = 100\ V$, the internal potential attains the maximum screening value $U_{int}^{out}(\mathbf{r}) = -83.40\ V$ at the interface, $\rho = a = 1\ \mu m$, in both cases. As we move radially, away from the cylinder-vacuum interface, the screening efficiency drops rapidly. However, now $U_{int}^{out}(\mathbf{r})$ attains an absolute value around 20% of $U_{ext}^{out}(\mathbf{r})$ within 1 μm from the interface for the case where $n = 1$ (panel (c)), while for $n = 2$ the respective absolute value is around 10% due to the influence that the higher value of the order, n, of $U_{ext}^{out}(\mathbf{r})$ has on $U_{int}^{out}(\mathbf{r})$ through the term $(a/\rho)^{2n}$, as discussed above.

Finally, the reader is invited to evaluate both the validity and easiness of our universal expressions by checking the solutions provided in the above two representative problems. To this end, the solutions should be found through standard approaches (e.g. using Poisson and Laplace equations, boundary conditions etc) that unavoidably go through time-consuming, lengthy algebraic calculations. Our approach has metabolized these calculations in advance, thus providing the final results in an effortless way through application of the universal expressions found in this work.

VI. Novelty, perspectives and limitations of the present work

The present work provides clear analytical expressions for the internal field and the polarization of a magnetic and dielectric cylinder that, ideally, has infinite length, subjected to an external field applied by the user. The external field can have any form on the plane normal to the axis of the cylinder, while it preserves translational invariance along the axis. Under these conditions the obtained expressions are universal and ready-to-use in all relevant cases. As was evidenced in the representative applications discussed above, by using these universal expressions we can obtain reliable results, quite effortlessly, in practically a single step. These results are identical to the ones obtained by other standard methodologies of electromagnetism that unavoidably should go through lengthy, time-consuming algebraic calculations in a step-by-step approach.

Our work has specific important findings that can be useful in realistic conditions, that is in experimental practice and in applications. First of all, we recall that here we consider a cylinder of infinite length, while in reality the assumption $L/a \gg 1$ holds, at best. It is expected that in this case, the two edges of the cylinder should have, practically, negligible contribution in comparison to that of its extended, central part. We stress that in experimental practice and in applications we always handle specimens of limited size, thus we are obliged to make some assumptions. Below we make a brief discussion mainly focused on magnetism. We clarify that our assumptions are reasonable, especially when compared to the ones commonly met in experimental practice and in applications that in most cases are crude or even, entirely, unjustified.

Regarding the experimental practice, when we use any kind of dc/ac magnetometer (such as SQUID, VSM, AC Susceptometer etc) to assess the magnetic properties of specimens, the specific shape and limited size of the specimen is not taken into account while processing the recorded responses. Specifically, the software of all commercial magnetometers, during the fitting of each recorded response, employs the very primitive model of an ideal, point-like, magnetic dipole to finally result in the magnetic moment/magnetization of the specimen on a quantitative basis [45,46]. Despite the fact that specimens are nor point-like (have finite dimensions), nor dipoles (higher order terms, such as quadrupole, can be present in the response), all commercial magnetometers use this very crude assumption. Our work makes a significant improvement in this respect. We have obtained theoretical expressions for the internal magnetic field (relation (45)) and the magnetization (relation (49)) of a cylinder for any form of the external magnetic field applied by the user on the plane normal to the cylinder's axis. Thus, our theoretical results can be used to fit experimentally recorded responses, referring to specimens consisting of cylinders that ideally should have infinite length. Nevertheless, we assume that our theoretical expressions still hold for realistic cylinders given that the condition $L/a \gg 1$ is satisfied, so that the cylinder seems to be infinite. Obviously, our results are much closer to reality when compared to the very crude assumption that cylinders (whether have infinite length or more realistically $L/a \gg 1$), behave as ideal, point-like dipoles. Thus, our theoretical work paves the way to a more reliable interpretation, both qualitatively and quantitatively, of experimental data obtained in magnetic cylinders.

Referring to applications, the magnetic cylinder is a model system in many respects. For instance, in the field of magnetophoresis, magnetic cylinders are met in various kinds of units in the form of wires that, indeed, satisfy the condition $L/a \gg 1$. Examples are the so-called single-wire and multi-wire magnetic separators [47-51]. In its simple version, this magnetophoretic unit consists of a single ferromagnetic wire [47], or a matrix of sparsely separated, non-interacting

ferromagnetic wires [48-51], that are subjected to an external magnetic field (most commonly, spatially homogeneous), applied normal to the directional axis. Each wire is magnetized by the external field, producing its internal field component. Accordingly, the total magnetic field becomes spatially inhomogeneous in close vicinity outside the surface of each wire. Importantly, all external, internal and total magnetic fields are homogeneous along the axis of the wire. Thus, the problem maintains translational invariance along this axis, so that, as discussed above, it is actually 2-dimensional (see Figures 1(a)-1(b)). On the contrary, on the plane normal to the axis of the wire the magnetic field is inhomogeneous resulting in a strong retention force that captures magnetic particles flowing inside a liquid medium [47-51]. Our work can be of interest in such devices for the detailed theoretical description of the underlying processes and the improvement of the overall retention efficiency. Specifically, in the basic version of these magnetic separators the external magnetic field applied by the user is homogeneous, while the inhomogeneity on the plane normal to the axis of the wires stems from their internal magnetic field. Our theoretical expressions can describe both easily and accurately the more complicate case where the external magnetic field is inhomogeneous, by default, on the plane normal to the axis of the wires (however, it should still preserve translational invariance along the directional axis). An inhomogeneous external magnetic field and the specific form of inhomogeneity (that is the employed specific mode(s)) can have significant impact on the retention force. For instance, the magnetophoretic units called quadrupole magnetic field flow fractionation (GMFFF), have the desired technical prescription [52-55]. These units are based on the introduction of an inhomogeneous magnetic field applied by a quadrupole electromagnet. The field is strongly inhomogeneous on the plane normal to the flow of a suspension of magnetic particles, while it preserves homogeneity along the axis of the flow [52-55]. Thus, using a GMFFF unit to apply a strongly inhomogeneous magnetic field on the plane normal to a single-wire or multi-wire building unit, could result in an efficient new device that probably has advanced characteristics. This hybrid device can still be described both easily and accurately by the theoretical expressions obtained in our work. Finally, in the field of electrophoresis, analogous separators exist that exhibit inhomogeneity on the plane normal to the building unit, while preserving homogeneity along its axis. For instance, a standard version is based on the coaxial configuration of a wire and a cylindrical shell, subjected to a potential difference. Such units are employed to precisely separate and capture charged nano/micro-particles [56-59]. Additional information on relevant magnetophoretic and electrophoretic units can be found in [55] and references therein.

The present work has some limitations. For instance, here we considered analytically a single magnetic and dielectric cylinder subjected to an external field. As discussed above, this building unit is met in many applications, such as the single-wire and multi-wire magnetic separators [47-51]. Obviously, our theoretical expressions fit ideally the single-wire case. A system of sparsely separated, non-interacting wires can, still, be easily studied following the same strategy. However, a system of densely packed, thus interacting wires, is more demanding. This situation is met in more complicate multi-wire magnetic separators based on a matrix of closely positioned wires [48-51]. More advanced theoretical approaches are needed to describe such units. Another limitation of our work stems from the inherent characteristics of the studied system. Specifically, our theoretical work describes systems that comprise of cylinders subjected to external fields that can exhibit any form of inhomogeneity on the plane normal to the cylinder's axis. However, both the cylinder and the external field should preserve translational invariance along the directional axis. Future theoretical works should explore more complicate systems that comprise of

cylinders and/or external fields with inhomogeneous characteristics even along the directional axis.

VII. Conclusions

We reported definite results on a linear, homogeneous and isotropic magnetic and dielectric cylinder of seemingly infinite length, subjected to an *external* (pseudo)potential/field, $\mathcal{U}_{ext}/\mathcal{F}_{ext}$, of *any* form on the plane normal to the directional axis, produced by a primary source that resides outside the cylinder. An expansion-based mathematical approach was employed, that enabled direct access to universal expressions of the response of the magnetic and dielectric cylinder, i.e. the *internal* (pseudo)potential/field, $\mathcal{U}_{int}/\mathcal{F}_{int}$, against the *external* ones, $\mathcal{U}_{ext}/\mathcal{F}_{ext}$. Ready-to-use expressions of the *total* (pseudo)potential/field, $\mathcal{U}=\mathcal{U}_{ext}+\mathcal{U}_{int}/\mathcal{F}=\mathcal{F}_{ext}+\mathcal{F}_{int}$, and of the polarization, $\mathcal{P}$, of the magnetic and dielectric cylinder were directly obtained, as well. The depolarization factor and the extrinsic susceptibility are degenerate since they obtain constant values, irrespectively of the mode of the applied $\mathcal{U}_{ext}/\mathcal{F}_{ext}$. These universal expressions between $\mathcal{U}_{int}$-$\mathcal{U}_{ext}$, $\mathcal{U}$-$\mathcal{U}_{ext}$, $\mathcal{F}_{int}$-$\mathcal{F}_{ext}$, $\mathcal{F}$-$\mathcal{F}_{ext}$ and $\mathcal{P}$-$\mathcal{F}_{ext}$ provide effective means to describe both analytically and computationally relevant systems.

CRediT

Petros Moraitis: Formal analysis, Investigation, Methodology, Writing – review & editing. Kosmas Tsakmakidis: Formal analysis, Investigation, Writing – review & editing, Funding acquisition. Dimosthenis Stamopoulos: Conceptualization, Data curation, Formal analysis, Investigation, Methodology, Supervision, Validation, Writing – original draft, Writing – review & editing.

Acknowledgment

P.M. and K.L.T. acknowledge funding within the frame work of the National Recovery and Resilience Plan Greece 2.0, funded by the European Union NextGenerationEU (Implementation body: HFRI), under Grant No. 16909. K.L.T. was also supported by the General Secretariat for Research and Technology and the Hellenic Foundation for Research and Innovation under Grant No. 4509.

Data Availability Statement

The data that supports the findings of this study are available within the article.

Conflicts of Interest

The authors declare that they have no known competing financial interests or personal relationships that could have appeared to influence the work reported in this paper.

References

1. Li X, Wang J and Zhang J 2021 *Sci. Rep.* **11** 20467 (doi: 10.1038/s41598-021-00124-w)
2. Loulas I, Zouros G P, Almpanis E and Tsakmakidis K L 2024 *IEEE International Symposium on Antennas and Propagation and INC/USNC-URSI Radio Science Meeting (AP-S/INC-USNC-URSI)* (doi: 10.1109/AP-S/INC-USNC-URSI52054.2024.10686607)
3. Peng L, Ran L, Chen H, Zhang H, Kong J A and Grzegorczyk T M 2007 *Phys. Rev. Lett.* **98** 157403 (doi: 10.1103/PhysRevLett.98.157403)

4. Wu Q, Zhang K, Meng F Y and Li L W 2010 *IET Microw. Antennas Propag.* **4** 1680 (doi: 10.1049/iet-map.2009.0256)
5. Akihiko I, Toshinobu S, Koji A and Tetsuya H 1991 *Bull. Inst. Chem. Res., Kyoto Univ.* **69** 421 (doi: http://hdl.handle.net/2433/77400)
6. Prodan E, Prodan C and Miller J H 2008 *Biophys. J.* **95** 4174 (doi: 10.1529/biophysj.108.137042)
7. Zehe A Ramírez A and Starostenko O 2004 *Braz. J. Med. Biol. Res.* **37** 173 (doi: 10.1590/S0100-879X2004000200003)
8. Green N G and Jones T B 2007 *J. Phys. D: Appl. Phys.* **40** 78 (doi: 10.1088/0022-3727/40/1/S12)
9. Ye H, Cotic M, Fehlings M G and Carlen P L 2011 *Med. Biol. Eng. Comput.* **49** 107 (doi: 10.1007/s11517-010-0704-0)
10. Spreng B, Berthoumieux H, Lambrecht A, Bitbol A F, Maia Neto P and Reynaud S 2024 *New J. Phys.* **26** 013009 (doi: 10.1088/1367-2630/ad1846)
11. Freake S M and Thorp T L 1971 *Rev. Sci. Instrum.* **42** 1411 (doi: 10.1063/1.1684894)
12. Ma H, Qu S, Xu Z, Zhang J, Chen B and Wang J 2008 *Phys. Rev. A* **77** 013825 (doi: 10.1103/PhysRevA.77.013825)
13. Xu J 2017 *AIP Advances* **7**, 125220 (doi: 10.1063/1.5010205)
14. Zhao Y and Su J 2019 *Chin. J. Phys.* **57** 14 (doi: 10.1016/j.cjph.2018.12.017)
15. Chu Y, Zhang X, Chen W, Wu F, Wang P, Yang Y, Tao S and Wang X 2019 *Sci. Total Environ.* **681** 124 (doi: 10.1016/j.scitotenv.2019.05.064)
16. Meng Y, Li C, Liu X, Lu J, Cheng Y, Xiao L P and Wang H 2019 *Sci. Total Environ.* **685** 847 (doi: 10.1016/j.scitotenv.2019.06.278)
17. Sieben S, Bergemann C, Lübbe A, Brockmann B and Rescheleit D 2001 *J. Magn. Magn. Mater.* **225** 175 (doi: 10.1016/S0304-8853(00)01248-8)
18. Furlani E P and Sahoo Y 2006 *J. Phys. D: Appl. Phys.* **39** 1724 (doi: 10.1088/0022-3727/39/9/003)
19. Gómez-Pastora J, Karampelas I H, Bringas E, Furlani E P and Ortiz I 2019 *Sci. Rep.* **9** 7265 (doi: 10.1038/s41598-019-43827-x)
20. Nasiri R, Shamloo A and Akbari J 2021 *Micromachines* **12** 877 (doi: 10.3390/mi12080877)
21. Bauer L A, Birenbaum N S and Meyer G J 2004 *J. Mater. Chem.* **14** 517 (doi: 10.1039/B312655B)
22. Reich D H, Tanase M, Hultgren A, Bauer L A, Chen C S and Meyer G J 2003 *J. Appl. Phys.* **93** 7275 (doi: 10.1063/1.1558672)
23. Cribb J A, Meehan T D, Shah S M, Skinner K and Superfine R 2010 *Ann. Biomed. Eng.* **38** 3311 (doi: 10.1007/s10439-010-0084-5)
24. Hultgren A, Tanase M, Chen C S, Meyer G J and Reich D H 2003 *J. Appl. Phys.* **93** 7554 (doi: 10.1063/1.1556204)
25. Karageorgou M A and Stamopoulos D 2021 *Sci. Rep.* **11** 9753 (doi: 10.1038/s41598-021-89117-3)
26. Stamopoulos D, Bouziotis P, Benaki D, Kotsovassilis C and Zirogiannis P N 2008 *Nephrol. Dial. Transplant.* **23** 3234 (doi: 10.1093/ndt/gfn189)
27. Zubarev A Yu, Abu-Bakr A F, Bossis G and Bulycheva S V 2014 *Magnetohydrodynamics* **50**, 397 (doi: 10.22364/mhd)
28. Abu-Bakr A F, Zubarev A Yu, 2019 *J. Magn. Magn. Mater.* **477**, 404 (doi: 10.1016/j.jmmm.2018.07.010)

29. Abu-Bakr A F, Zubarev A Yu 2020 *Eur. Phys. J. Special Topics* **229**, 2991 (doi: 10.1140/epjst/e2020-000054-1)
30. Wang C, Wang X, Anderson S W and Zhang X 2014 *Sens. Actuators B Chem.* **196** 670 (doi: 10.1016/j.snb.2014.01.096)
31. Tay Z W *et al.* 2018 *ACS Nano* **12** 3699 (doi: 10.1021/acsnano.8b00893)
32. Hournkumnuard K and Natenapit M 2013 *Med. Phys.* **40** 06230 (doi: 10.1118/1.4805097)
33. Jackson J D 1998 *Classical Electrodynamics* 3rd edn (Wiley)
34. Zangwill A 2013 *Modern Electrodynamics* 1st edn (Cambridge University Press: Cambridge)
35. Stamopoulos D 2024 *Materials* **17** 5046 (doi: 10.3390/ma17205046)
36. Stamopoulos D 2025 *Crystals* **15** 331 (doi: 10.3390/cryst15040331)
37. Sandim M J R, Sandim H R Z, Stamopoulos D, Renzetti R A, Das Virgens M G and Ghivelder L 2006 *IEEE Trans. Appl. Supercond.* **16** 1692 (doi: 10.1109/TASC.2005.864287)
38. Stamopoulos D, Pissas M, Sandim M J R and Sandim H R Z 2006 *Physica C* **442** 45 (doi: 10.1016/j.physc.2006.04.019)
39. Kittel C 2005 *Introduction to Solid State Physics* 8th edn (John Wiley & Sons)
40. Prozorov R and Kogan V G 2018 *Phys. Rev. Applied* **10** 014030 (doi: 10.1103/PhysRevApplied.10.014030)
41. Coey J M D 2010 *Magnetism and Magnetic Materials* Illustrated edn (Cambridge University Press: Cambridge)
42. Skomski R, Hadjipanayis G C and Sellmyer D J 2007 *IEEE Trans. Magn.* **43** 2956 (doi: 10.1109/TMAG.2007.893798)
43. Arfken G B, Weber H J and Harris F E 1985 *Mathematical Methods for Physicists* 7th edn (Academic Press: Cambridge).
44. Joslin C G and Gray C G 1983 *Mol. Phys.* **50** 329 (doi: 10.1080/00268978300102381)
45. Lewis L H and Bussmann M K 1996 *Rev. Sci. Instrum.* **67** 3537 (doi: 10.1063/1.1147172)
46. Coak M J, Liu C, Jarvis D M, Park S, Cliffe M J, Goddard P A 2020 *Rev. Sci. Instrum.* **91** 023901 (doi: 10.1063/1.5137820)
47. Khan M B, Rassolov P, Ali J, Siegrist T, Humayun M, Mohammadigoushki H 2025 *J. Chem. Phys.* **163** 024903 (doi: 10.1063/5.0269000)
48. Ahmed N, Jiang Y, Wang A, Xue Z and Chen L 2024 *Sep. Sci. Technol.* **60** 351 (doi: 10.1080/01496395.2024.2426013)
49. Jiang Y, Zeng J, Cao M, Yu W, Xie E, Chen L 2024 *Physicochem. Probl. Miner. Process.* **60** 183620 (doi: 10.37190/ppmp/183620)
50. Ye F, Deng H, Guo Z, Wei B, Ren X 2023 *Results Phys.* **49** 106482 (doi: 10.1016/j.rinp.2023.106482)
51. Zeng J, Tong X, Yi F, Chen L 2019 *Minerals* **9** 509 (doi:10.3390/min9090509)
52. Carpino F, Moore L R, Chalmers J J, Zborowski M and Williams P S 2005 *J. Phys.: Conf. Ser.* **17** 174 (doi:10.1088/1742-6596/17/1/024)
53. Carpino F, Moore L R, Zborowski M, Chalmers J J and Williams P S 2005 *J. Magn. Magn. Mater.* **293** 546 (doi: 10.1016/j.jmmm.2005.01.071)
54. Williams P S, Carpino F and Zborowski M 2009 *Mol. Pharm.* **6** 1290 (doi: 10.1021/mp900018v)
55. Lan Z, Chen R, Zou D, Zhao C X 2025 *Adv. Sci.* **12** 2411278 (doi: 10.1002/advs.202411278)
56. Liu L *et al.* 2022 *Anal. Chem.* **94** 8474−8482 (doi: 10.1021/acs.analchem.2c01313)
57. Xie P, Yang X, Fatima Z, Yang R, Sun H, Xing Y, Xu X, Gu J, Liu L and Li D 2024 *Anal. Chim. Acta* **1287** 342110 (doi: 10.1016/j.aca.2023.342110)

58. Xing Y *et al.* 2025 *Anal. Chem.* **97** 436−443 (doi: 10.1021/acs.analchem.4c04560)
59 Liu L, Cui J, Chen P, Fatima Z, Xing Y, Liu H, Ren X and Li D 2024 *J. Chromatogr. A* **1727** 464990 (doi: 10.1016/j.chroma.2024.464990)